Electronic supporting Information

Chiral recognition coupled with chemometrics using boronate ensembles containing D-π-A cyanostilbenes

Kaede Kawaguchi, Ayana Moro, Soya Kojima and Yuji Kubo*

Department of Applied Chemistry, Graduate School of Urban Environmental Sciences, Tokyo Metropolitan University, 1-1 Minami-Osawa, Hachioji, Tokyo 192-0397, Japan

Contents

General

NMR spectra were measured on a Bruker Avance 500 MHz NMR spectrometer (^{1}H: 500 MHz, ^{13}C: 126 MHz), JEOL 400 MHz NMR spectrometer (^{11}B: 128 MHz), and JEOL 300 MHz NMR spectrometer (^{1}H: 300 MHz). In ^{1}H and ^{13}C NMR measurements, chemical shifts (δ) are reported downfield from the internal standard Me_4Si. ^{11}B NMR chemical shift was referenced to external $BF_3 \cdot Et_2O$. Electrospray ionization (ESI) mass spectrum was recorded on Bruker micrOTOF II-SDT1 spectrometer. The absorption and emission were measured using Shimadzu UV-3600 UV/vis/NIR spectroscopy and JASCO FP-8500 spectrofluorometers, respectively. Quantum yields in THF solution and solid were measured by FP-8500 with an integrating sphere unit (JASCO ILF-835 100 mm ϕ) and an integrating sphere unit (JASCO ISF-834 60 mm ϕ), respectively. Powder X-ray diffraction (PXRD) data were collected by a Rigaku RINT-TTR III X-ray diffractometer with Cu Kα radiation. DLS were performed by an ELSZ-2 (OTSUKA ELECTRONICS) instrument. Density functional theory (DFT) calculations at the M062X/6-31+G(d,p) level were performed in the Gaussian 16 software.[1] These molecular orbitals were visualized using Gauss view 6.0.16 program.

Materials

Unless otherwise indicated, reagents used for the synthesis were commercially available and were used as supplied. (Z)-3-(4-(diphenylamino)phenyl)-2-(4-pinacolborylphenyl)acrylonitrile (**1**)[2] and 2-(4-diphenylamino)phenyl)acetonitrile (**2**)[3] were prepared according to methods previously reported.

Synthesis

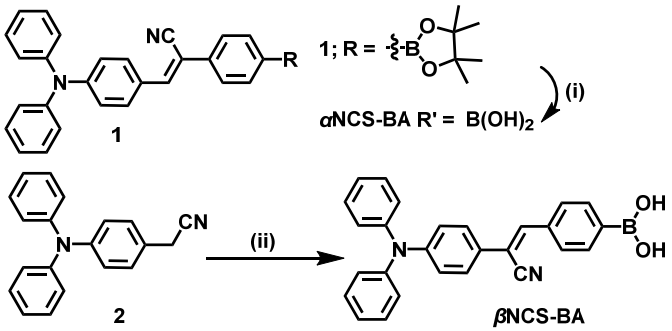

(Z)-3-(4-(diphenylamino)phenyl)-2-(4-dihydroxyborylphenyl)acrylonitrile (*α*NCS-BA)

To a solution of **1** (0.950 g, 1.91 mmol) in THF (20 mL) under a N_2 condition was added 2.1 mL of aqueous solution of KHF_2 (0.744 g, 9.53 mmol) at room temperature. The resultant mixture was stirred for 5 h at room temperature, quenched by water and evaporated to give 0.927 g of the solid as a yellow solid. It then was dissolved in THF (15 mL) and H_2O (3 mL). To the solution was added an aqueous solution of $LiOH \cdot H_2O$ (0.320 g, 7.62 mmol) in H_2O (14 mL). The mixture was tired for 3.5 h at room temperature. After the reaction was quenched by pouring H_2O, the resultant solution was neutralized with 1N HCl aqueous solution, evaporated and then extracted with EtOAc. The organic layer was evaporated and reprecipitated with THF and hexane. 0.463 g of ***α*NCS-BA** was obtained in 58% yield, in which 3 % of E-isomer was contained.

^{1}H NMR (500 MHz, DMSO-d_6): δ (ppm) = 8.15 (s, 2H), 7.95 (s, 1H), 7.88 (d, 2H, J = 8.10 Hz), 7.87 (d, 2H, J = 8.80 Hz), 7.69 (d, 2H, J = 8.20 Hz), 7.40 (t, 4H, J = 7.82 Hz), 7.18 (t, 4H, J = 7.45 Hz), 7.15 (d, 2H, J = 7.75 Hz), 6.96 (d, 2H, J = 8.85 Hz). ^{1}H NMR (300 MHz, THF-d_8): δ (ppm) = 7.87 (d, 2H, J = 8.79 Hz), 7.85 (d, 2H, J = 8.28 Hz), 7.71 (s, 1H), 7.67 (dt, 2H, J = 8.28, 1.66 Hz), 7.31 (ddt, 4H, J = 8.14, 7.61, 2.39 Hz), 7.26 (s, 2H), 7.15 (dt, 4H, J = 7.23, 1.34 Hz), 7.10 (tt, 2H, J = 7.29, 1.30 Hz), 7.03 (dt, 2H, J = 9.15, 2.31 Hz). ^{13}C NMR (126 MHz, DMSO-d_6): δ (ppm) = 149.5, 146.0, 142.3, 135.6, 134.8, 130.8, 129.9, 126.1, 125.6, 124.7, 124.3, 120.0, 118.5, 106.3. ^{11}B NMR (128 MHz, THF-d_8): δ (ppm) = 27.80. HRMS (ESI-MS): calcd for $C_{27}H_{21}BN_2O_2$: 416.1695, Found: 416.1727 $[M]^+$. Elemental analysis: calcd (%) for $C_{27}H_{21}BN_2O_2 \cdot 0.3H_2O$: C 78.93, H 5.00, N 6.82, Found: C 79.07, H 4.98, N 7.01.

***(Z)*-2-(4-(diphenylamino)phenyl)-4-(4-dihydroxyborylphenyl)acrylonitrile (*β*NCS-BA)**

Compound (**2**) (1.38 g, 4.84 mmol), 4-formylphenylboronic acid (0.806 g, 5.37 mmol) and NaOH (1.91 g, 47.8 mmol) were dissolved in EtOH (40 mL) under a N_2 atmosphere. The resultant mixture was refluxed for 20 h at 85 °C, and then neutralized with NH_4Cl and 1M HCl aqueous solution. After filtration, the solid was chromatographed on silica gel (Wacogel C-300) using a gradient of CH_2Cl_2 (75 – 0% v/v) in AcOEt, washed with CH_2Cl_2 and recrystallized with CH_3CN and H_2O. In this way, 0.459 g of ***β*NCS-BA** was obtained in 22% yield.

^{1}H NMR (500 MHz, DMSO-d_6): δ (ppm) = 8.20 (s, 2H), 7.89 (d, J = 8.15 Hz, 2H), 7.89 (s, 1H), 7.85 (d, J = 8.10 Hz, 2H), 7.65 (dt, J = 9.25, 2.47 Hz, 2H), 7.36 (ddt, J = 8.18, 7.78, 2.29 Hz, 4H), 7.13 (tt, J = 7.40, 1.13 Hz, 2H), 7.09 (dd, J = 8.55, 1.00 Hz, 2H), 7.02 (dt, J = 9.30, 2.47 Hz, 2H). ^{1}H NMR (300 MHz, THF-d_8): δ (ppm) = 7.87 (s, 4H), 7.64 (s, 1H), 7.60 (d, 2H, J = 8.67 Hz), 7.30 (s, 2H), 7.28 (t, 4H, J = 7.83 Hz), 7.10 (d, 4H, J = 8.31 Hz), 7.07 (d, 2H, J = 9.15 Hz), 7.05 (t, 2H, J = 7.77 Hz). ^{13}C NMR (126 MHz, DMSO-d_6): δ (ppm) = 148.28, 146.51, 140.54, 135.29, 134.44, 129.73, 127.79, 126.98, 124.78, 123.96, 121.93, 117.92, 110.19. ^{11}B NMR (128 MHz, THF-d_8): δ (ppm) 28.51. HRMS (ESI-MS): calcd for $C_{27}H_{21}BN_2O_2$ 416.1695, 417.1774, found 416.1714 $[M]^+$, 417.1759 $[M+H]^+$. Elemental analysis calcd. (%) for $C_{27}H_{21}BN_2O_2 \cdot 0.3H_2O$: C 76.90, H 5.16, N 6.64, Found: C 76.86, H 5.05, N 6.59.

X-ray crystallographic analysis of *β*NCS-BA

A suitable single crystal of ***β*NCS-BA** obtained by recrystallization was subject to X-ray crystallographic analysis (CCDC No. 2109188), which belong to P−1 space group with Z = 2. The Oak Ridge thermal ellipsoid plot (ORTEP) diagram is presented in Fig. S1.

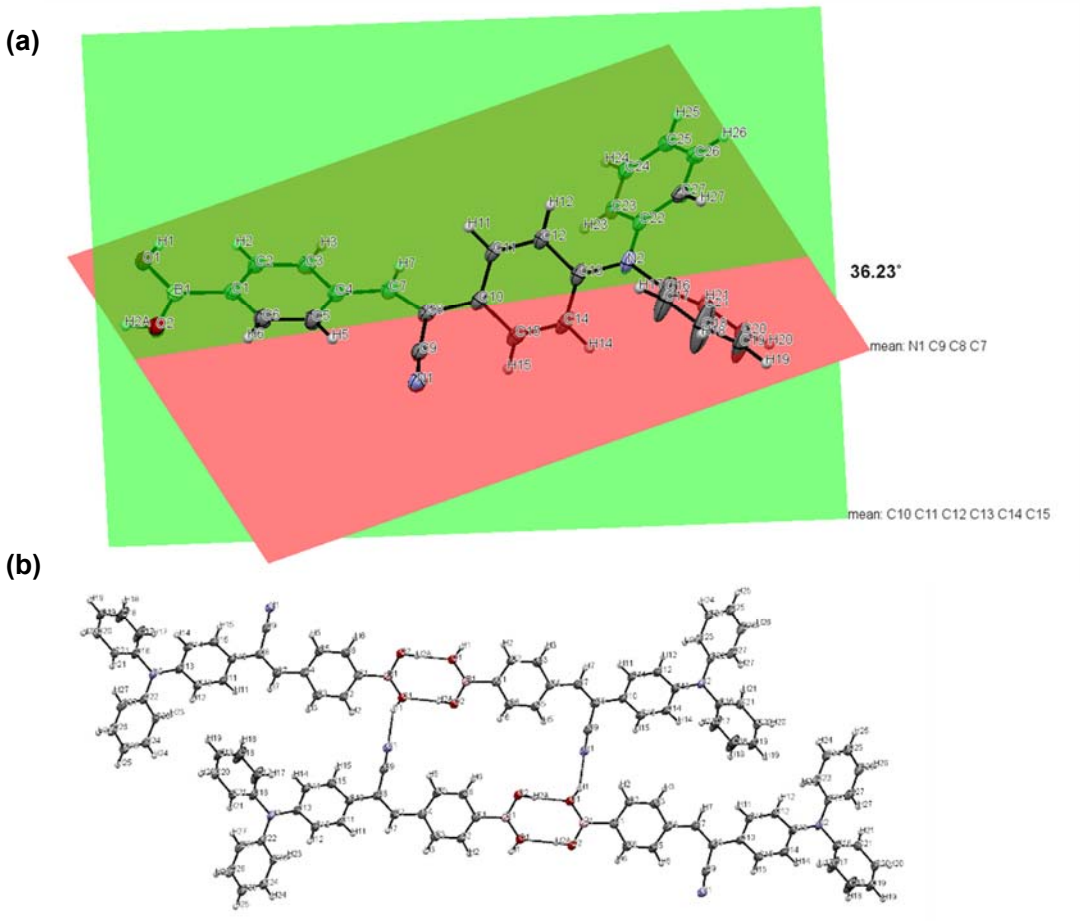

Fig. S1. X-ray crystal structure of ***β*NCS-BA** where (a) thermal ellipsoids are drawn at 50% probably level and (b) packing structure.

Lippert-Mataga plot

$$\Delta f = \frac{D-1}{2D+1} - \frac{n^2-1}{2n^2+1} \qquad \tilde{\nu}_{\mathrm{abs}} - \tilde{\nu}_{\mathrm{em}} = \Delta f \frac{2(\mu_{\mathrm{E}} - \mu_{\mathrm{G}})^2}{hcr^3} + const.$$

The Δf is the orientational polarisability where D and n are dielectric constant and refractive index, respectively. The parameters of h, c and r are the Plank's constant, the velocity of light, and the Onsager radius r, respectively. DFT calculation (M062X/6-31+G(d,p)) was used to estimate r (***α*NCS-BA**: 6.16 Å, ***β*NCS-BA**: 6.10 Å). Linear relationships between the Stokes shift ($\tilde{\nu}_{\mathrm{abs}} - \tilde{\nu}_{\mathrm{em}}$) and Δf was obtained (Fig. S2) to afford the difference between excited- and ground-state dipole moments.

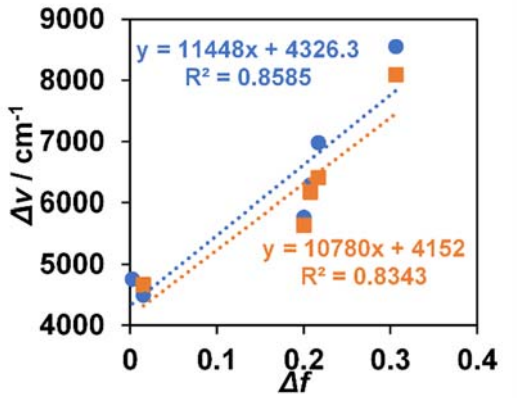

Fig. S2. Lippert-Mataga plots of ***α*NCS-BA** (■) and ***β*NCS-BA** (●).

Aggregation-induced emission properties of *α*NCS-BA and *β*NCS-BA

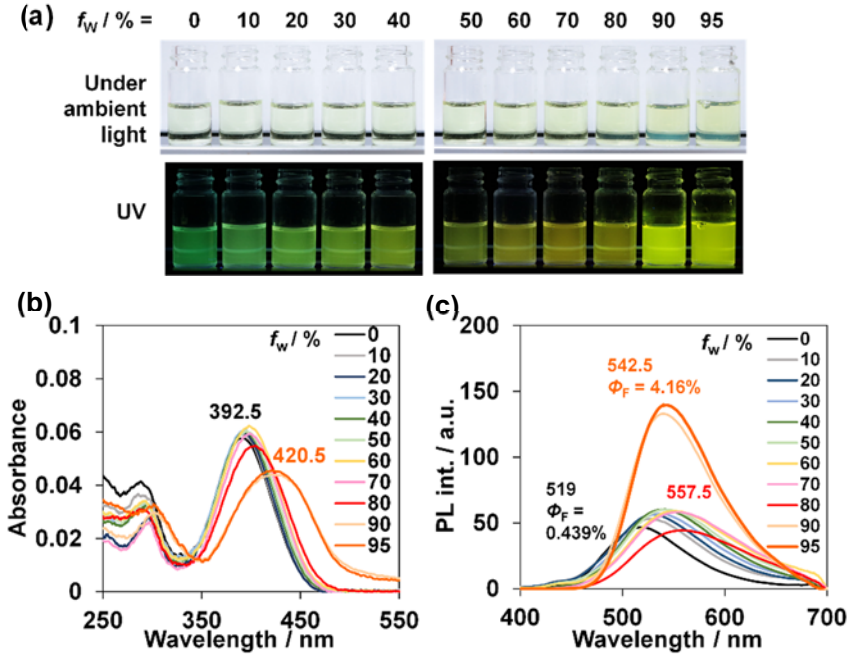

Fig. S3. AIE properties of ***α*NCS-BA** (20 μM) in THF/H_2O mixture containing different volume fraction of water; (a) Images under UV 365 lamp, (b) UV/Vis absorption spectra and (c) emission spectra. λ_{em} = 365 nm.

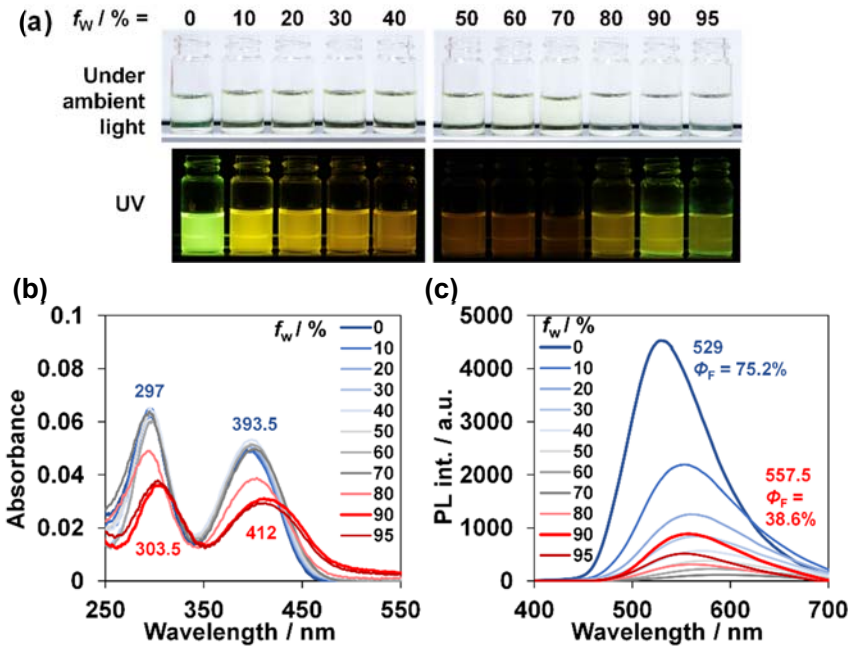

Fig. S4. AIE properties of ***β*NCS-BA** (20 μM) in THF/H_2O mixture containing different volume fraction of water; (a) Images under UV 365 lamp, (b) UV/Vis absorption spectra and (c) emission spectra. λ_{em} = 365 nm.

Preparation of boronate ensembles

(4*S*,5*S*)-2-(4-((Z)-1-cyano-2-(4-(*N*,*N*-diphenylamino)phenyl)vinyl)phenyl-1,3,2-dioxaborolane-4,5-dicarboxylic acid (L-*α*NCS-TA)

***α*NCS-BA** (3.07 mg, 7.49×10^{-3} mmol) and L-tartaric acid (1.13 mg, 7.53×10^{-3}mmol) were dissolved in THF-d_8 under N_2 atmosphere (10 mM). The resultant mixture was shaken for 5 h at room temperature in the presence of molecular sieves 4A.

^{1}H NMR (300 MHz, THF-d_8): δ (ppm) = 11.81 (brd, 2H), 7.90 (d, 2H, J = 8.07 Hz), 7.89 (d, 2H, J = 8.91 Hz), 7.77 (s, 1H), 7.75 (d, 2H, J = 8.28 Hz), 7.32 (t, 4H, J = 7.77 Hz), 7.16 (d, 4H, J = 7.92 Hz), 7.11 (t, 2H, J = 7.64 Hz), 7.03 (d, 2H, J = 8.76 Hz), 5.06 (s, 2H). ^{11}B NMR (128 MHz, THF-d_8): δ (ppm) = 30.32. HRMS (ESI-MS in the negative mode): calcd for $C_{31}H_{23}BN_2O_6$ 529.1571, found 529.1573 $[M-H]^-$.

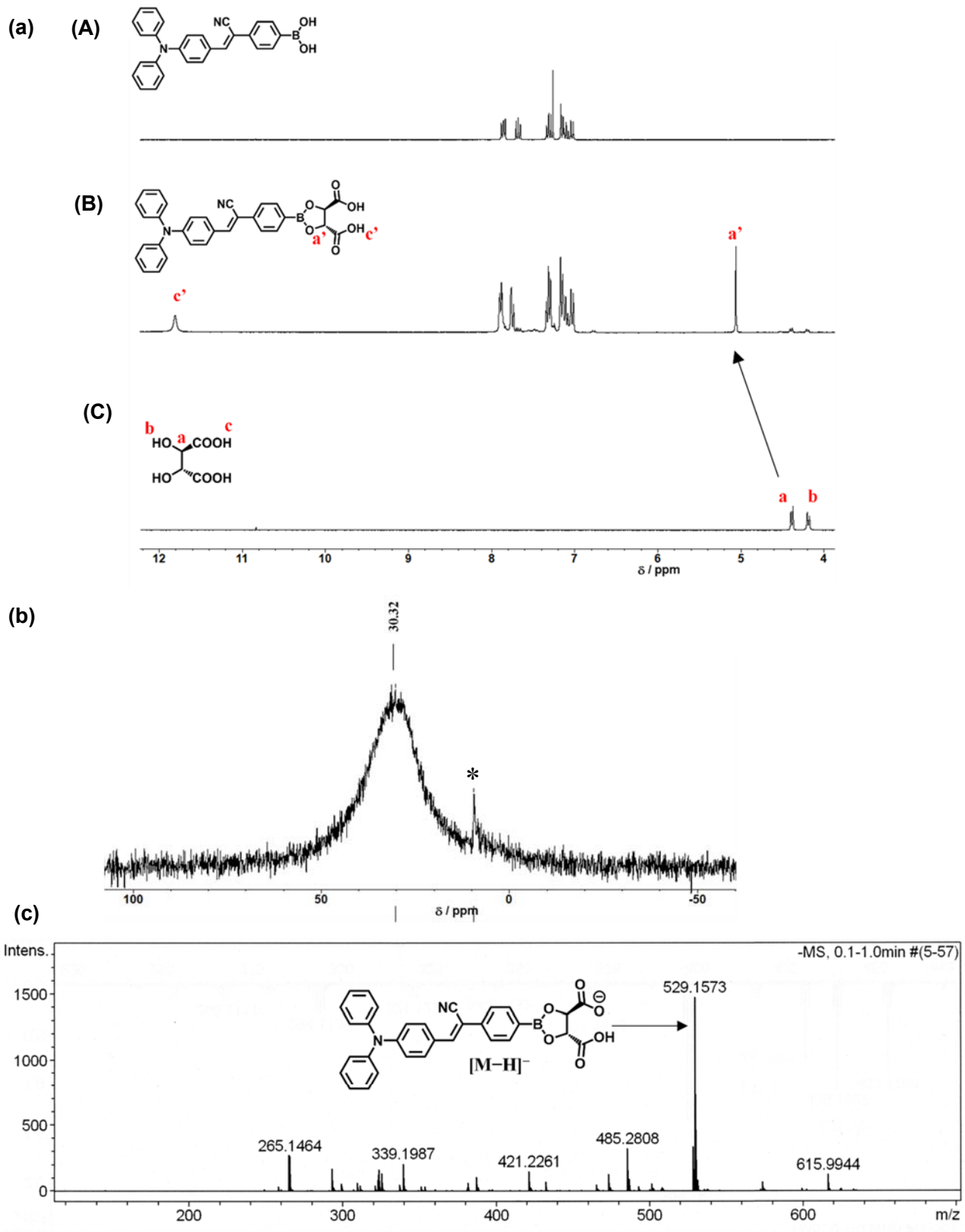

Fig. S5. (a) ^{1}H NMR (300 MHz, THF-d_8, room temperature) spectra: (A) ***α*NCS-BA** (20 mM). (B) After aging the mixture of L-tartaric acid (10 mM) and ***α*NCS-BA** (10 mM) for 5 h. (C) L-tartaric acid (20 mM). (b) ^{11}B NMR (128 MHz, THF-d_8, room temperature) spectrum of a mixture of L-tartaric acid (25 mM) and ***α*NCS-BA** (25 mM) for 5 h. The peak (*) at 9.39 ppm may be due to unidentified impurity. (c) HR MS (ESI-MS in the negative mode).

Preparation of other ensembles

These were prepared in a similar manner as L-***α*NCS-TA**.

(4*R*,5*R*)-2-(4-((Z)-1-cyano-2-(4-(*N*,*N*-diphenylamino)phenyl)vinyl)phenyl-1,3,2-dioxaborolane-4,5-dicarboxylic acid (D-*α*NCS-TA)

^{1}H NMR (300 MHz, THF-d_8): δ (ppm) = 11.81 (brd, 2H), 7.90 (d, 2H, J = 8.25 Hz), 7.89 (d, 2H, J = 8.82 Hz), 7.77 (s, 1H), 7.75 (d, 2H, J = 8.28 Hz), 7.32 (t, 4H, J = 7.78 Hz), 7.16 (d, 4H, J = 7.65 Hz), 7.11 (t, 2H, J = 7.57 Hz), 7.03 (d, 2H, J = 8.76 Hz), 5.06 (s, 2H). HRMS (ESI-MS in the negative mode): calcd for $C_{31}H_{23}BN_2O_6$ 529.1571, found 529.1568 $[M-H]^-$.

(4*S*,5*S*)-2-(4-((Z)-2-cyano-2-(4-(*N*,*N*-diphenylamino)phenyl)vinyl)phenyl-1,3,2-dioxaborolane-4,5-dicarboxylic acid (L-*β*NCS-TA)

^{1}H NMR (300 MHz, THF-d_8): δ (ppm) = 11.85 (brd, 2H), 7.93 (s, 4H), 7.68 (s, 1H), 7.62 (d, 2H, J =8.76 Hz), 7.28 (t, 4H, J = 7.52 Hz), 7.12−7.04 (m, 8H), 5.08 (s, 2H). ^{11}B NMR (128 MHz, THF-d_8): δ (ppm) = 31.07. HRMS (ESI-MS in the negative mode): calcd for $C_{31}H_{23}BN_2O_6$ 529.1571, found 529.1578 $[M-H]^-$.

(4*R*,5*R*)-2-(4-((Z)-2-cyano-2-(4-(*N*,*N*-diphenylamino)phenyl)vinyl)phenyl-1,3,2-dioxaborolane-4,5-dicarboxylic acid (D-*α*NCS-TA)

^{1}H NMR (300 MHz, THF-d_8): δ (ppm) = 11.75 (brd, 2H), 7.93 (s, 4H), 7.68 (s, 1H), 7.62 (d, 2H, J =8.73 Hz), 7.28 (t, J = 7.73 Hz), 7.03-7.12 (m), 5.07 (s, 2H). HRMS (ESI-MS in the negative mode): calcd for $C_{31}H_{23}BN_2O_6$ 529.1571, found 529.1560 $[M-H]^-$.

Table S1. Fluorescence quantum yields in THF solutions ($\Phi_{F,s}$) and of the as-prepared solids ($\Phi_{F,aps}$), and AIE factor (α_{AIE}) of ***α*NCS-BA** or ***β*NCS-BA**.

	$\Phi_{F,s}$ / % (THF solution)	$\Phi_{F,aps}$ / % (solid)[a]	α_{AIE}[b]
***α*NCS-BA**	0.439	2.57	5.85
***β*NCS-BA**	75.2	40.2	0.535

[a]The as-prepared solids were obtained by reprecipitation with THF/H_2O. [b]AIE factor ($\alpha_{AIE} = \Phi_{F,aps}/\Phi_{F,s}$).

Chiral sensing behavior of L-*α*NCS-TA toward enantiomeric CHDAs

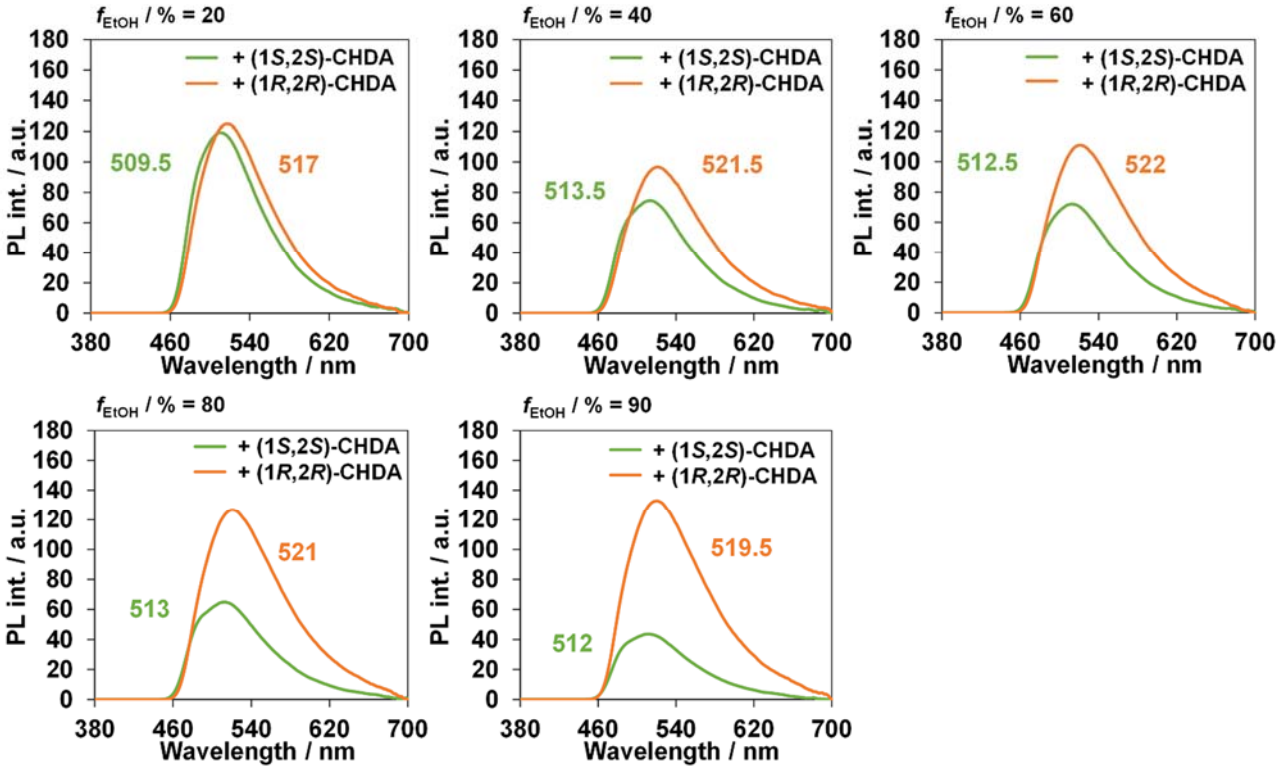

Fig. S6. Emission spectra of L-***α*NCS-TA** (0.75 mM) with (1*S,2S*)-**CHDA** or (1*R,2R*)-**CHDA** (0.75 mM) in THF/EtOH with different EtOH fraction. λ_{ex} = 365 nm. 25 °C.

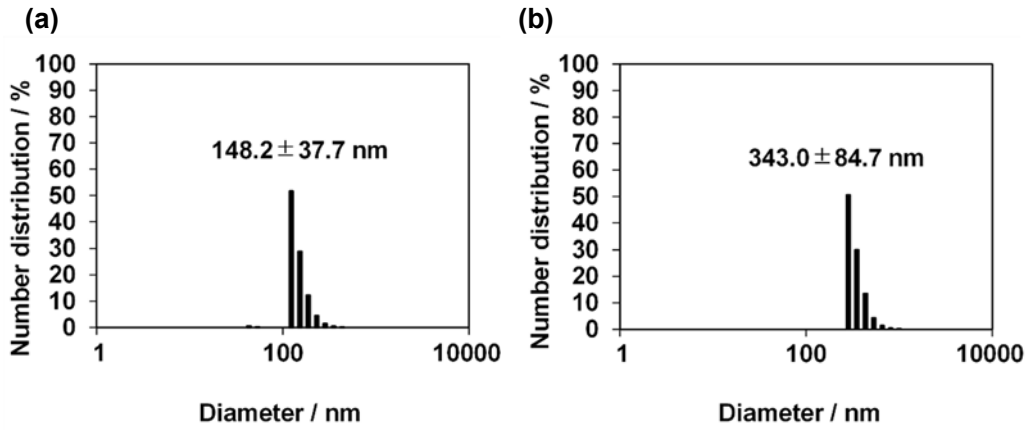

Fig. S7. DLS spectra of dispersed solutions of (a) L-***α*NCS-TA** (0.70 mM) with (1*S,2S*)-**CHDA** (0.70 mM) and (b) L-***α*NCS-TA** (0.70 mM) with (1*R,2R*)-**CHDA** (0.70 mM).

Chiral sensing behavior of L-*β*NCS-TA toward enantiomeric CHDAs

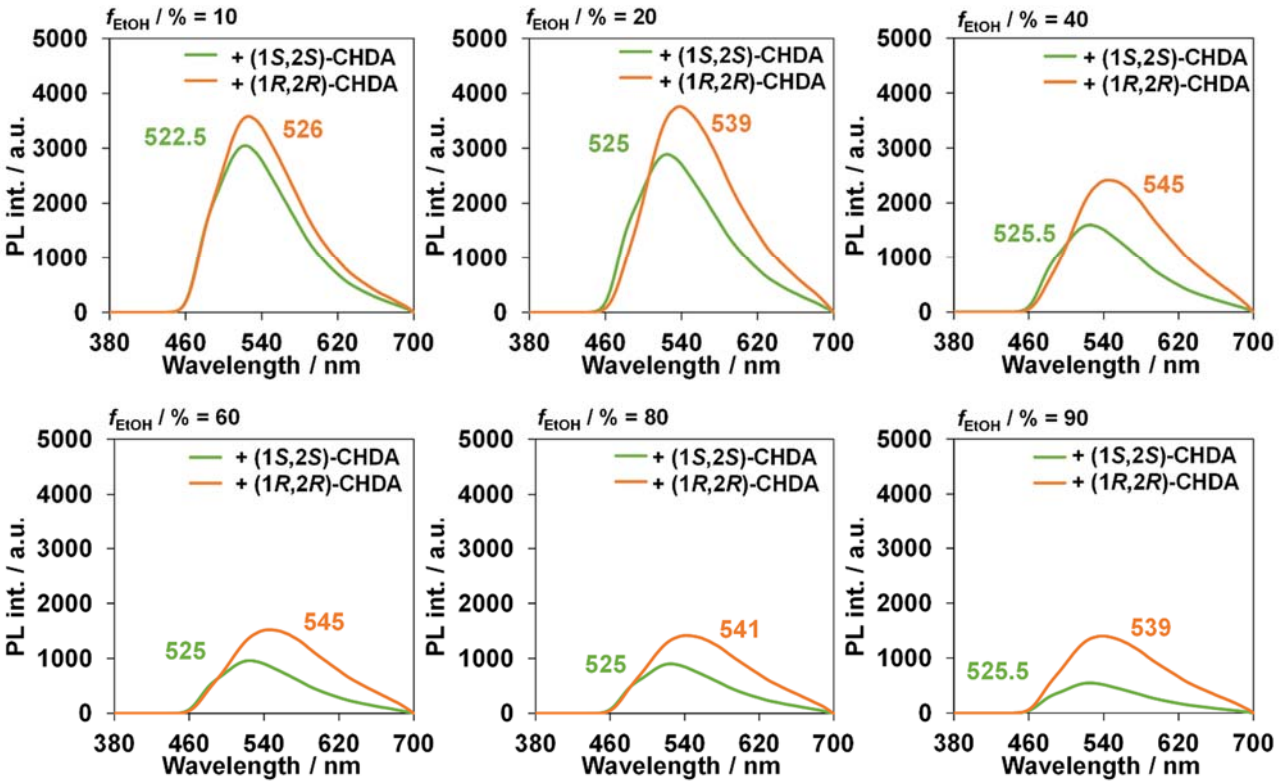

Fig. S8. Emission spectra of L-***β*NCS-TA** (0.75 mM) with (1*S,2S*)-**CHDA** or (1*R,2R*)-**CHDA** (0.75 mM) in THF/EtOH with different EtOH fraction. λ_{ex} = 365 nm. 25 °C.

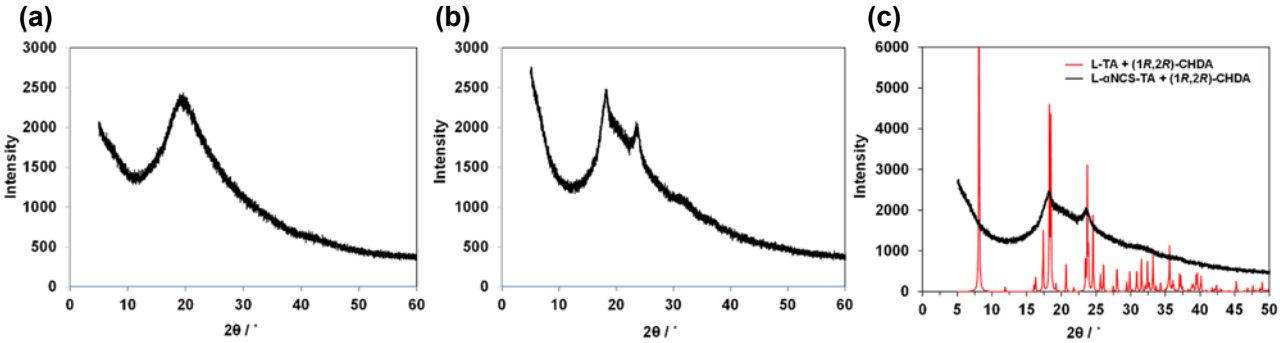

Fig. S9. PXRD patterns of L-***α*NCS-TA** with (a) (1*S,2S*)-**CHDA** or (b) (1*R,2R*)-**CHDA**. (c) Simulated PXRD pattern based on (1*R*,2*R*)-**CHDA** and L-tartaric acid (red solid line) and PXRD patterns of L-***α*NCS-TA** with (1*R,2R*)-**CHDA** (black solid line).

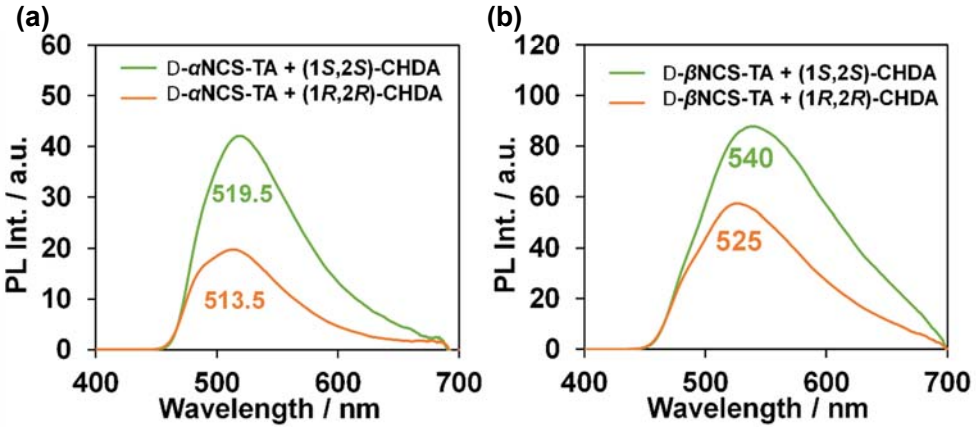

Fig. S10. Fluorescence spectra of (a) D-***α*NCS-TA** (0.75 mM) with enantiomers of **CHDA** (0.75 mM) in THF/EtOH (1:9 v/v) and (b) D-***β*NCS-TA** (0.75 mM) with enantiomers of **CHDA** (0.75 mM) in THF/EtOH (1:4 v/v).

Analysis procedure of linear discriminant analysis (LDA) and artificial neural network (ANN) models

Before the discrimination, the input data was prepared by the deconvolution of each spectrum by pseudo-Voigt function (*eq.* 1) as shown in Fig. S11.

$$V(x) = A\left\{p\exp\left(-\frac{(x-\mu)^2}{2\sigma^2}\right) + (1-p)\left(\frac{\sigma^2}{(x-\mu)^2+\sigma^2}\right)\right\} \quad (1)$$

Where A is amplification, p is Gaussian fraction, μ is peak position, σ is peak width. Those four fitted parameters were used as the input data of our LDA and artificial neural network (ANN) models.

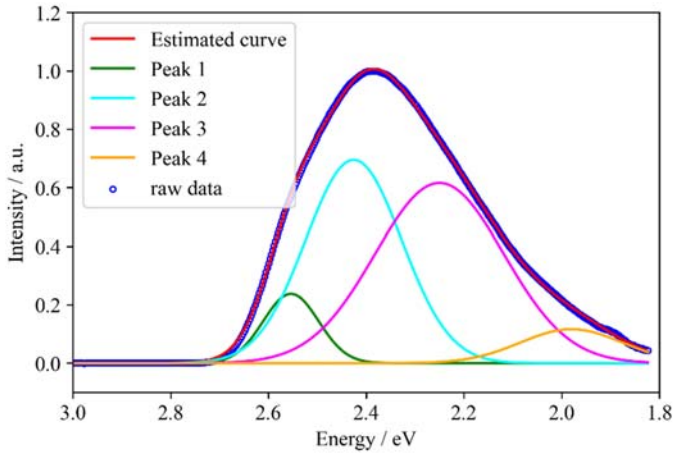

Fig. S11. Result of the spectrum peak fittings of L-***α*NCS-TA**+(1*R*,2*R*)-**CHDA**.

Table S2. Confusion matrix of LDA.

			Estimated class			
			Training data		Test data	
			1*R*,2*R*	1*S*,2*S*	1*R*,2*R*	1*S*,2*S*
Actual class	Training data	1*R*,2*R*	46	0	0	0
		1*S*,2*S*	0	46	0	0
	Test data	1*R*,2*R*	0	0	11	0
		1*S*,2*S*	0	0	0	11
	Total		46	46	11	11

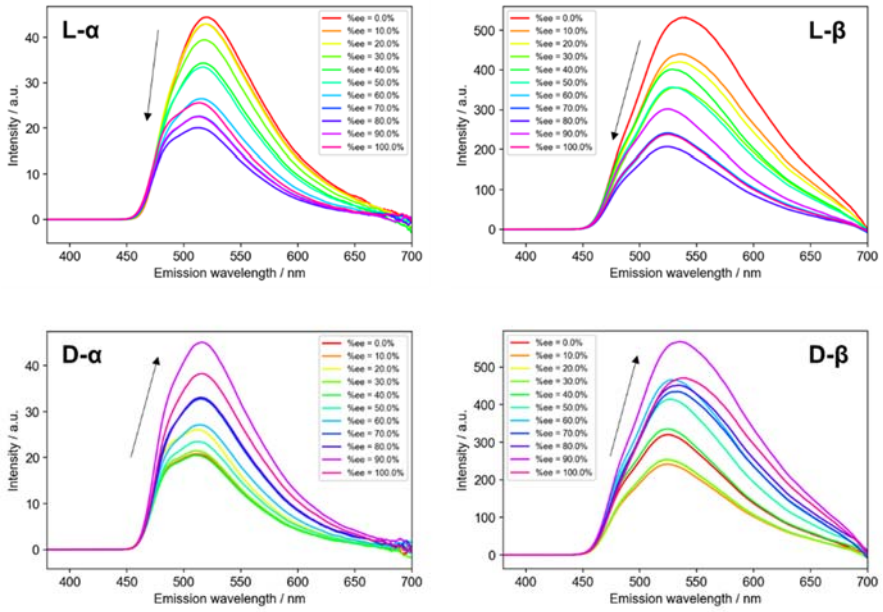

Fig. S12. Emission spectra of (a) L-***α*NCS-TA**, (b) L-***β*NCS-TA**, (c) D-***α*NCS-TA** and (d) D-***β*NCS-TA** as a function of %ee values of (1*R*,2*R*)-**CHDA** at f_{EtOH} of 80 % in EtOH/THF mixture.

Analysis method of neural network

We made 14,256 pattern combinations of the fitted parameters of L-***α*NCS-TA**, L-***β*NCS-TA**, D-***α*NCS-TA** and D-***β*NCS-TA** with the same enantiomer excess of (1*R*,2*R*)-**CHDA**. Note that, only the samples with 80% of f_{EtOH}, 25°C of measurement temperature, and 365 nm of λ_{ex} were used for %ee estimation and prediction, to reduce the dispersion of spectral data and improve the regression precision. Furthermore, 80% of the entire data was used for training, and another 20% was used as test data. As to creating a better model, hyperparameters of the ANN model were optimized by 5-fold grid search cross-validation. The network configuration of our ANN model is shown in Fig. S13. Mean-squared error (MSE) was used as a loss function, and Adaptive Moment Estimation (Adam) with 5×10^{-4} of learning rate was used for the optimization algorithm. L2 regularization term was introduced in two dense layers to avoid overfitting. Hence, the cost function of our model can be described as below (eq. 2).

$$\text{Cost function} = \frac{1}{n}\sum_{i=1}^{n}(\boldsymbol{y}_i - \boldsymbol{w}^{\mathrm{T}}\boldsymbol{x}_i)^2 + \lambda\|\boldsymbol{w}\|_2^2 \qquad (2)$$

Where, $\boldsymbol{y}_i$ is the objective variable, $\boldsymbol{x}_i$ is the explanatory variable, $\boldsymbol{w}$ is the weight vector, and λ is the weight of L2 regularization (in this case, 0.0002).

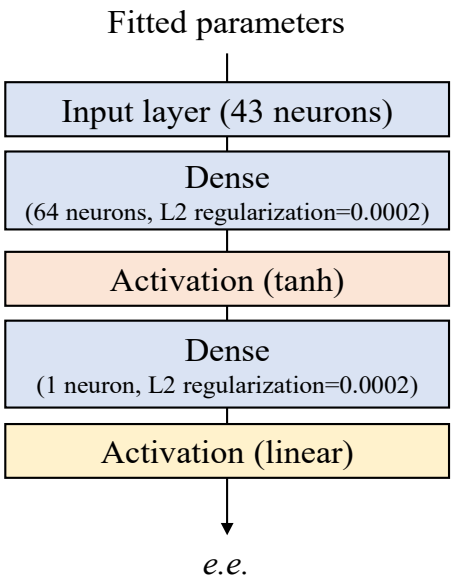

Fig. S13. Structure of our ANN model.

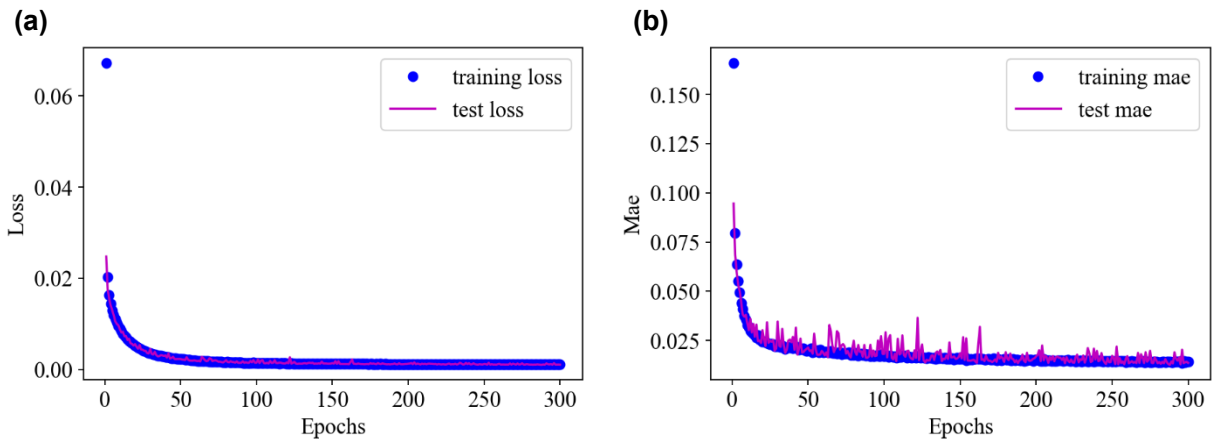

Fig. S14. (a) Loss function and (b) MAE changes against the learning epochs.

Table S3. Predicted enantiomer excesses and its error of the out-of-sample prediction data.

Sample no.	f_{EtOH} / %	λ_{ex} / nm	Actual ee / %	Predicted ee / %	Error / %
1	80	365	60.00	69.71	9.41
2	80	365	0.00	3.27	3.27
3	80	365	−60.00	−61.60	−1.60

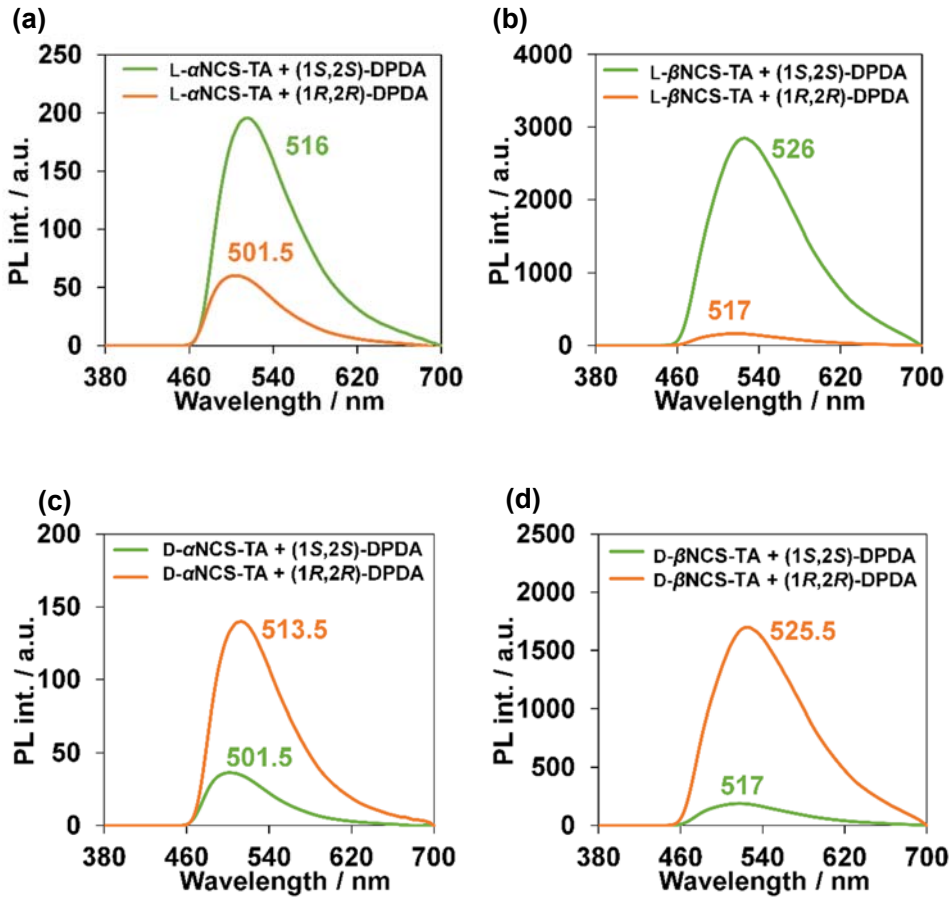

Fig. S15. Fluorescence spectra of (a) L-***α*NCS-TA** with chiral **DPDA**, (b) L-***β*NCS-TA** with chiral **DPDA**, (c) D-***α*NCS-TA** with chiral **DPDA** and (d) D-***β*NCS-TA** in THF/2-PrOH (3:17 v/v). [L-***α*NCS-TA**] = [L-***β*NCS-TA**] = [D-***α*NCS-TA**] = [D-***β*NCS-TA**] = 1.50 mM, [(1*S*,2*S*)-**DPDA**] = [(1*R*,2*R*)-**DPDA**] = 2.25 mM. λ_{ex} = 365 nm. 25 °C.

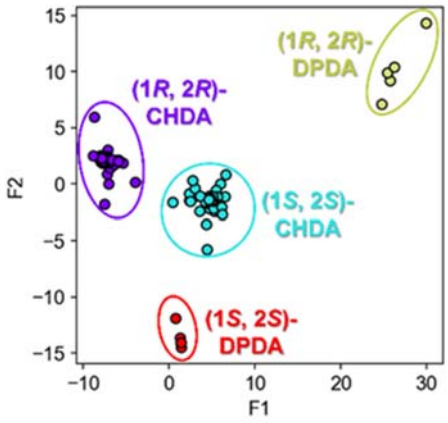

Fig.S16. LDA canonical plots for the analysis of two types of enantiomers pairs of amines.

References

1. M. J. Frisch, G. W. Trucks, H. B. Schlegel, G. E. Scuseria, M. A. Robb, J. R. Cheeseman, G. Scalmani, V. Barone, G. A. Petersson, H. Nakatsuji, X. Li, M. Caricato, A. V. Marenich, J. Bloino, B. G. Janesko, R. Gomperts, B. Mennucci, H. P. Hratchian, J. V. Ortiz, A. F. Izmaylov, J. L. Sonnenberg, D. Williams-Young, F. Ding, F. Lipparini, F. Egidi, J. Goings, B. Peng, A. Petrone, T. Henderson, D. Ranasinghe, V. G. Zakrzewski, J. Gao, N. Rega, G. Zheng, W. Liang, M. Hada, M. Ehara, K. Toyota, R. Fukuda, J. Hasegawa, M. Ishida, T. Nakajima, Y. Honda, O. Kitao, H. Nakai, T. Vreven, K. Throssell, J. J. A. Montgomery, J. E. Peralta, F. Ogliaro, M. J. Bearpark, J. J. Heyd, E. N. Brothers, K. N. Kudin, V. N. Staroverov, T. A. Keith, R. Kobayashi, J. Normand, K. Raghavachari, A. P. Rendell, J. C. Burant, S. S. Iyengar, J. Tomasi, M. Cossi, J. M. Millam, M. Klene, C. Adamo, R. Cammi, J. W. Ochterski, R. L. Martin, K. Morokuma, O. Farkas, J. B. Foresman and D. J. Fox, Revision A.03 ed., Gaussian, Inc., 2016.
2. S. Zeng, L. Yin, C. Ji, X. Jiang, K. Li, Y. Li and Y. Wang, *Chem. Commun.*, 2012, **48**, 10627-10629.
3. Y. Li, F. Shen, H. Wang, F. He, Z. Xie, H. Zhang, Z. Wang, L. Liu, F. Li, M. Hanif, L. Ye and Y. Ma, *Chem. Mater.*, 2008, **20**, 7312-7318.

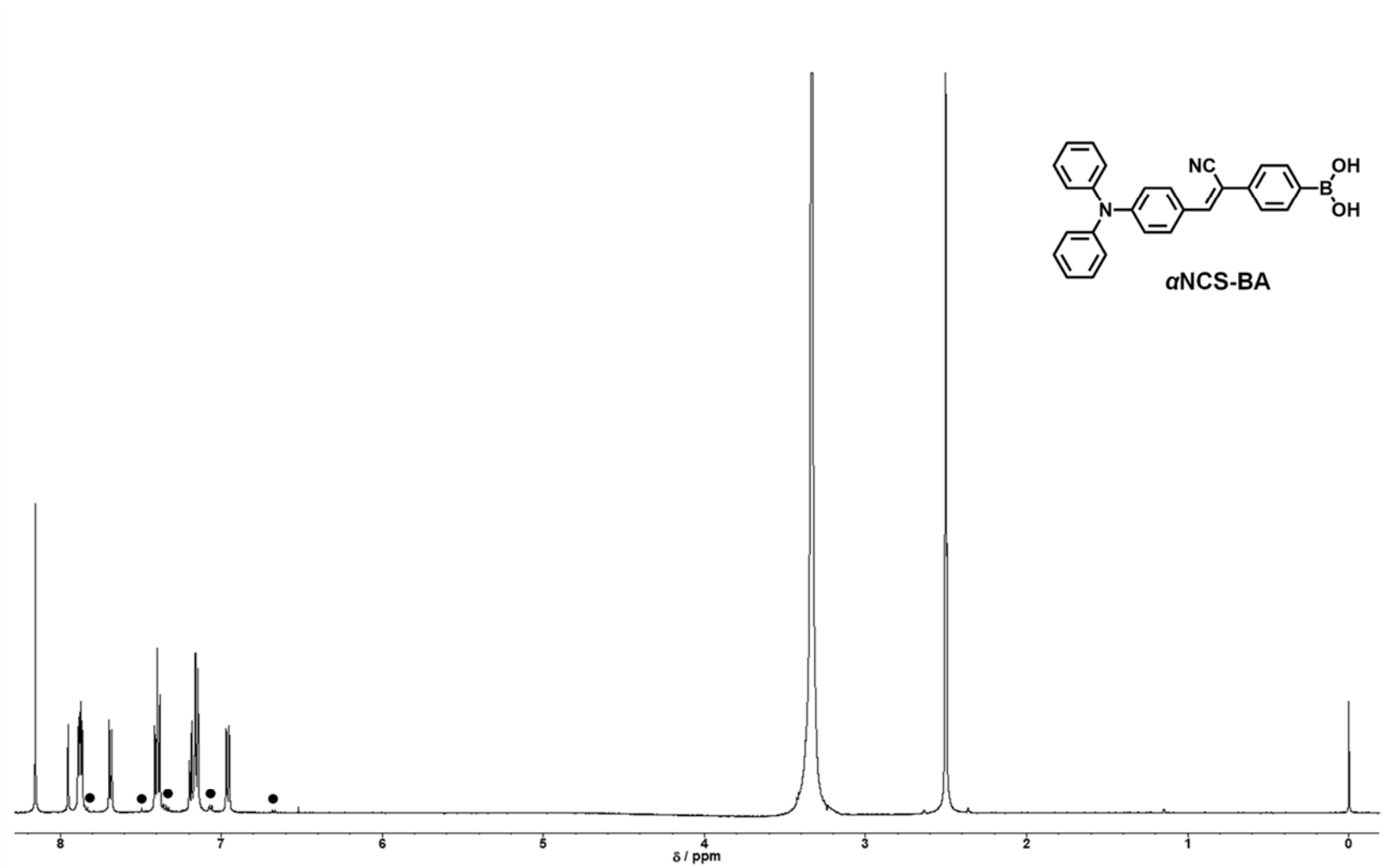

Fig. S17. ^{1}H NMR spectrum (500 MHz) of ***α*NCS-BA** in DMSO-d_6. Small signals (●) were from E-isomer ***α*NCS-BA**.

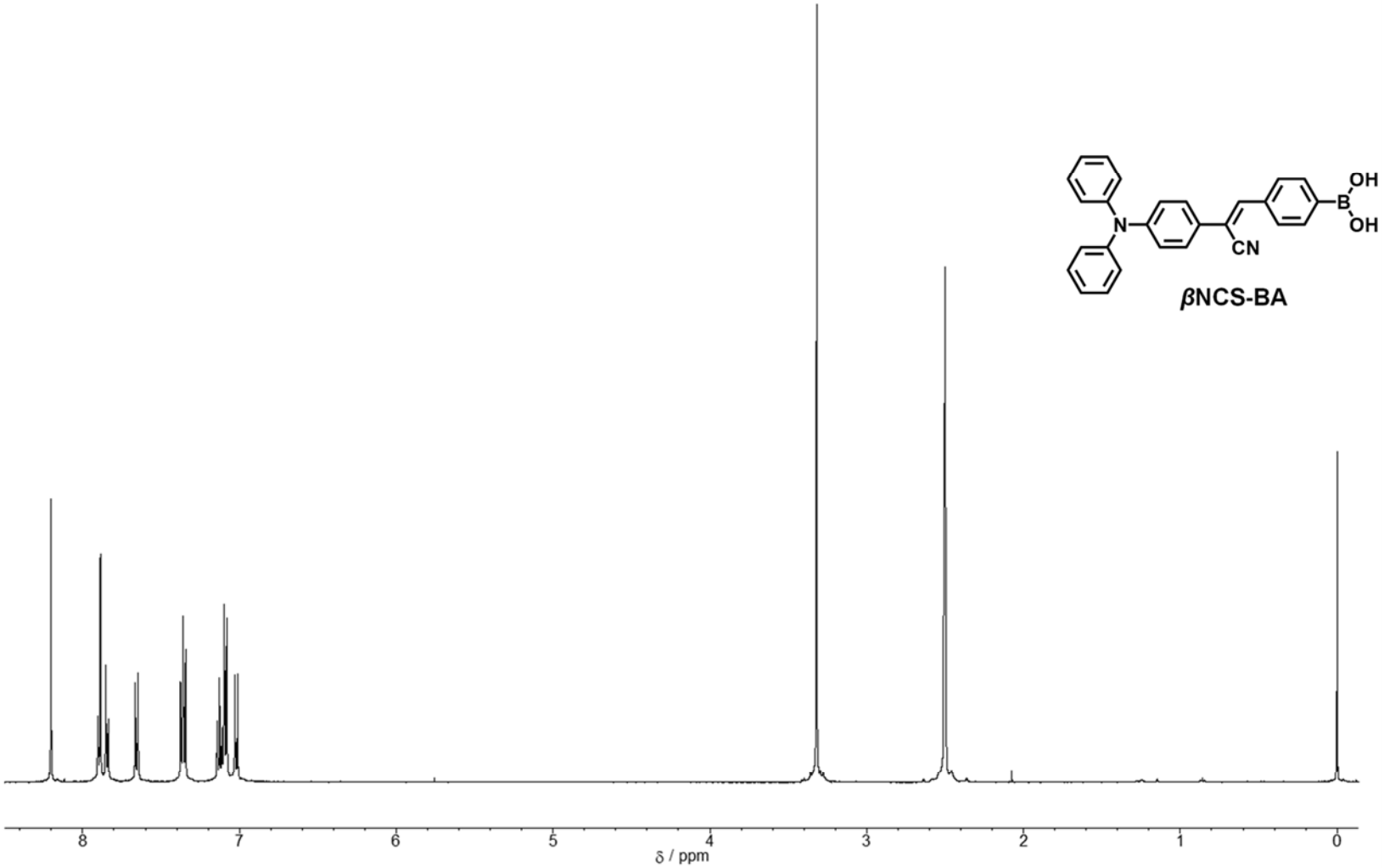

Fig. S18. ^{1}H NMR spectrum (500 MHz) of ***β*NCS-BA** in DMSO-d_6.

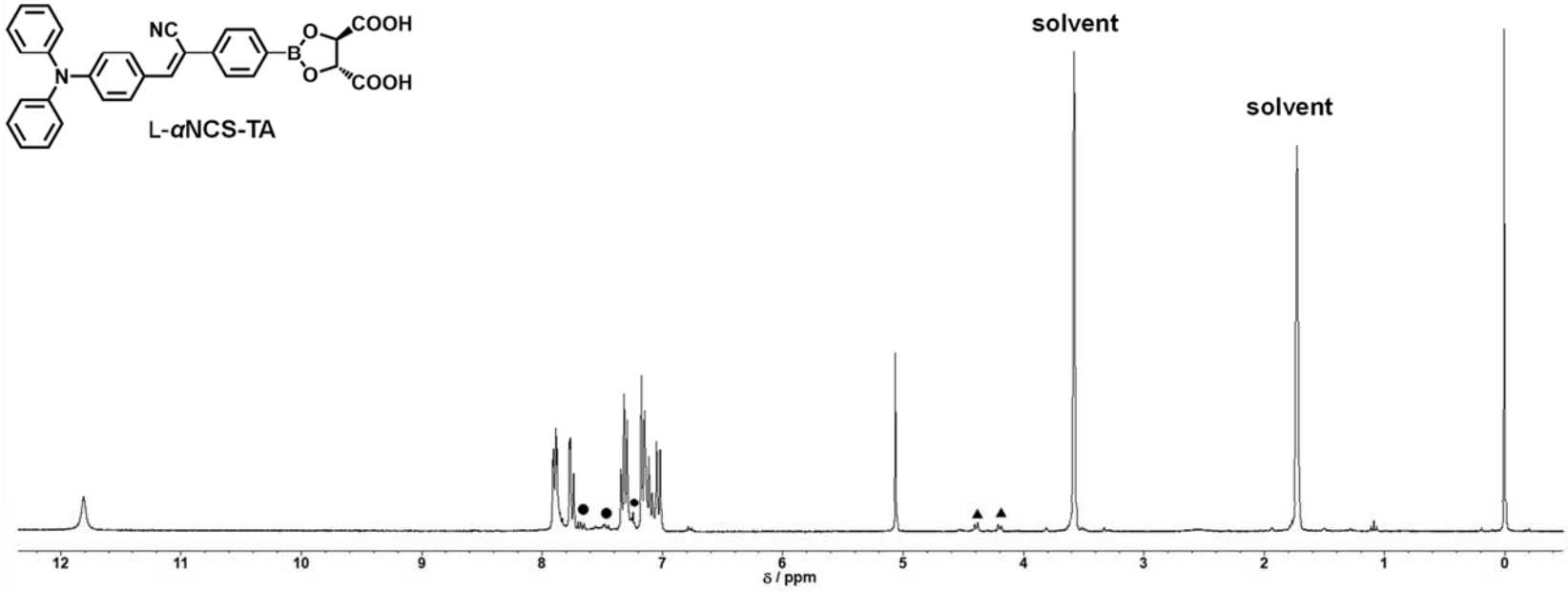

Fig. S19. [1]H NMR spectrum (300 MHz) of L-***α*NCS-TA in THF-d_8. The signals arising from residual ***α*NCS-BA** (●) and L-tartaric acid (▲) were detected.

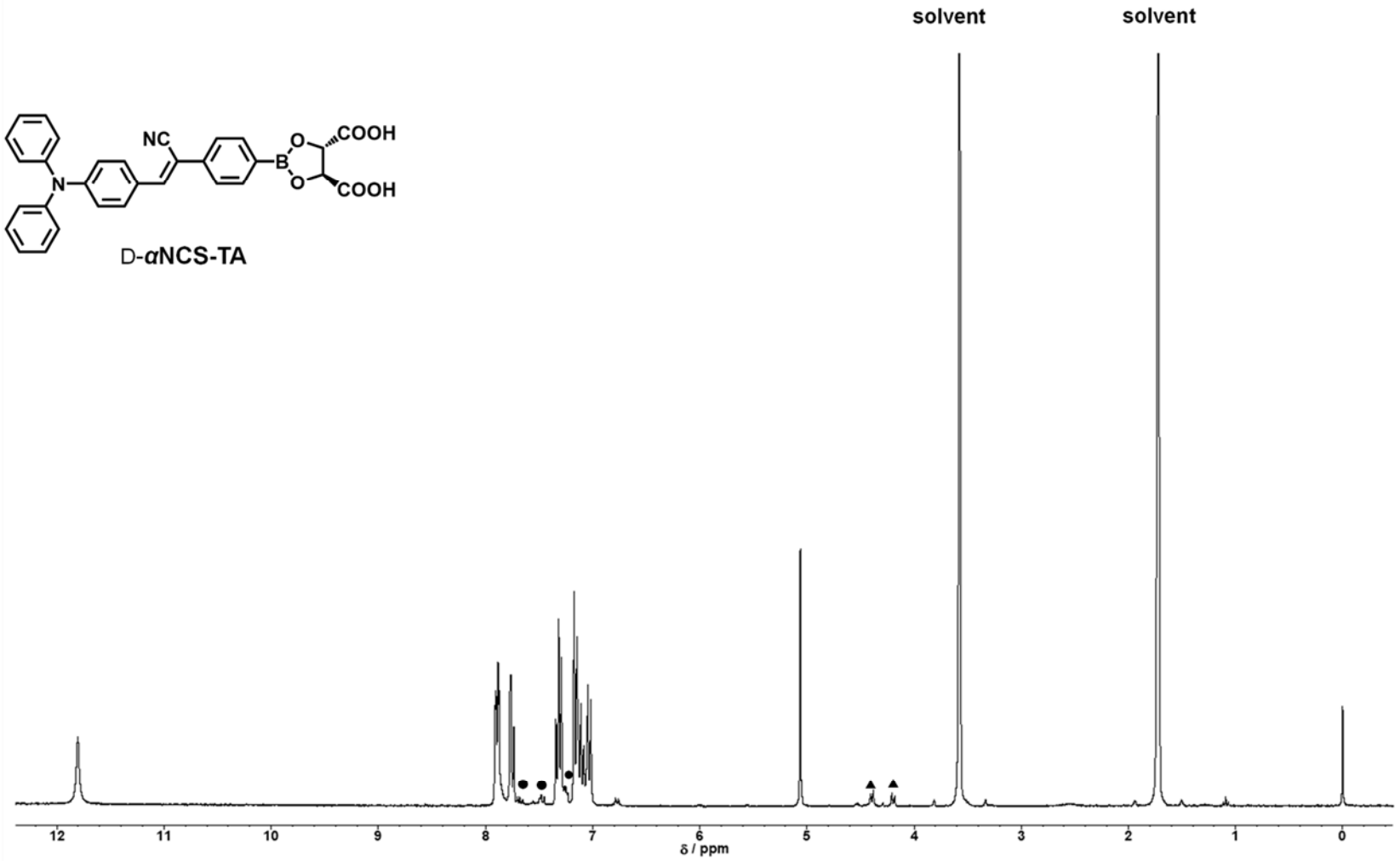

Fig. S20. [1]H NMR spectrum (300 MHz) of D-***α***NCS-TA** in THF-d_8. The signals arising from residual ***α*NCS-BA** (●) and D-tartaric acid (▲) were detected.

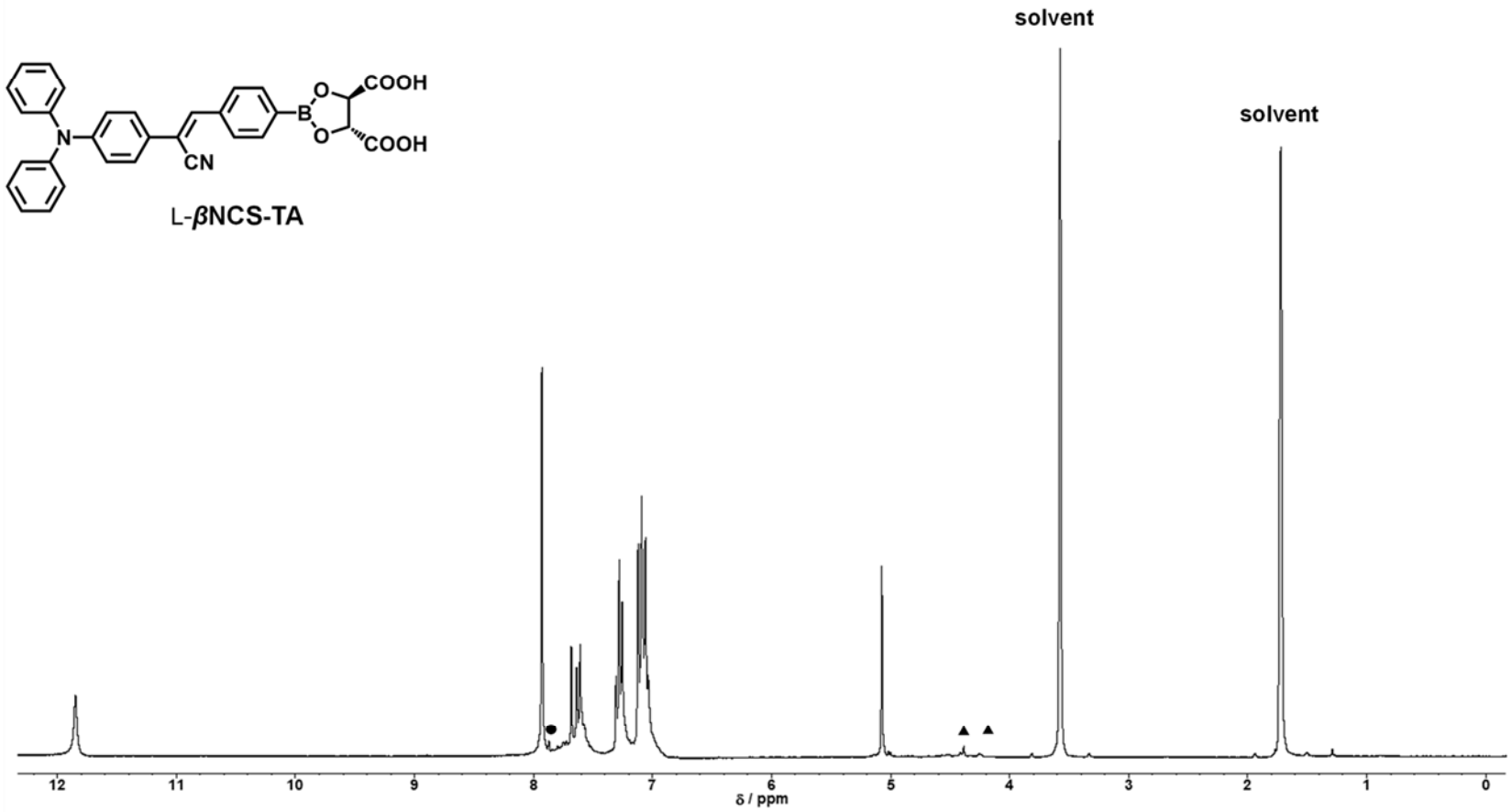

Fig. S21. ^{1}H NMR spectrum (300 MHz) of L-***β*NCS-TA in THF-d_8. The signals arising from residual ***β*NCS-BA** (●) and L-tartaric acid (▲) were detected.

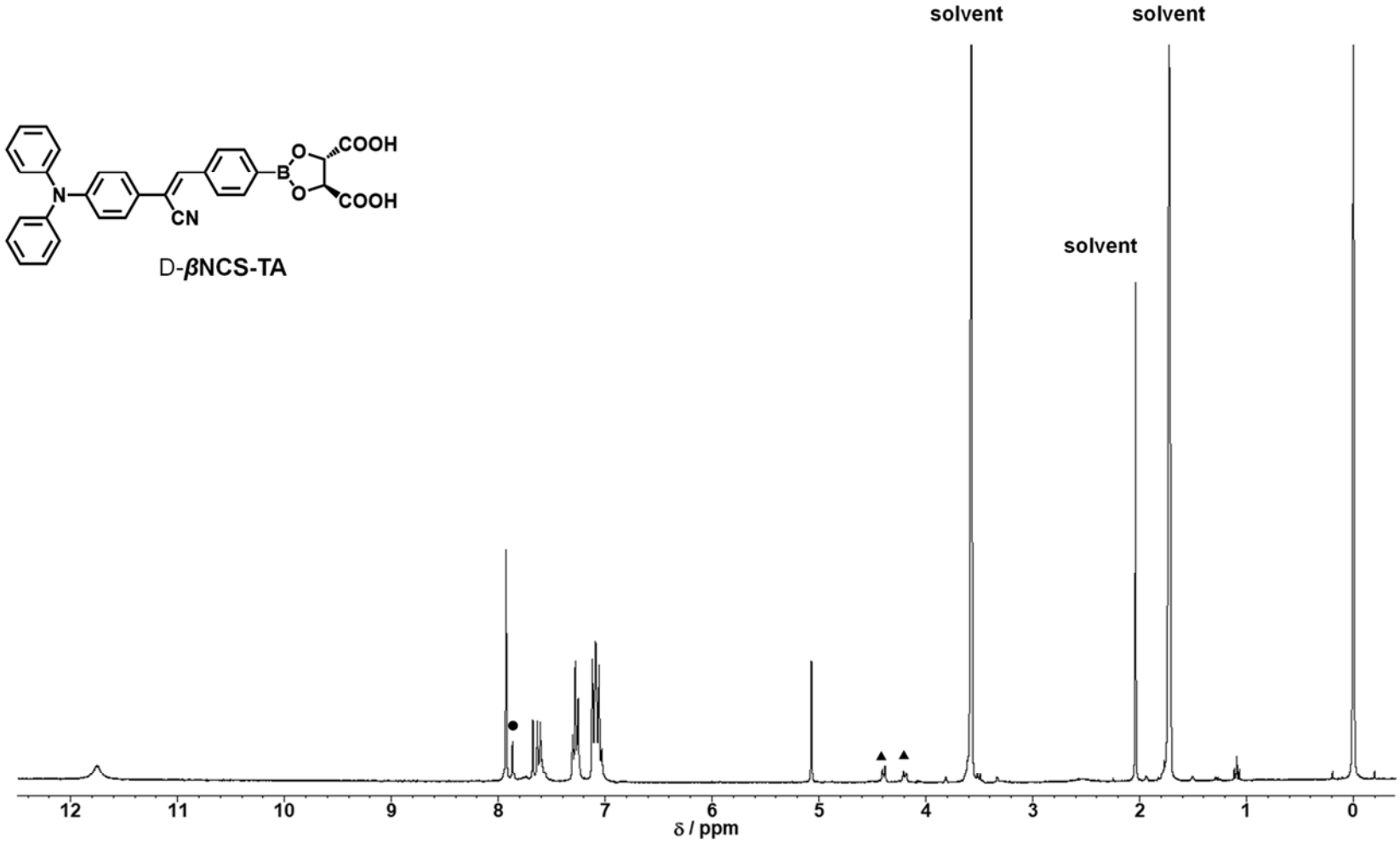

Fig. S22. ^{1}H NMR spectrum (300 MHz) of D-***β***NCS-TA** in THF-d_8. The signals arising from residual ***β*NCS-BA** (●) and D-tartaric acid (▲) were detected.

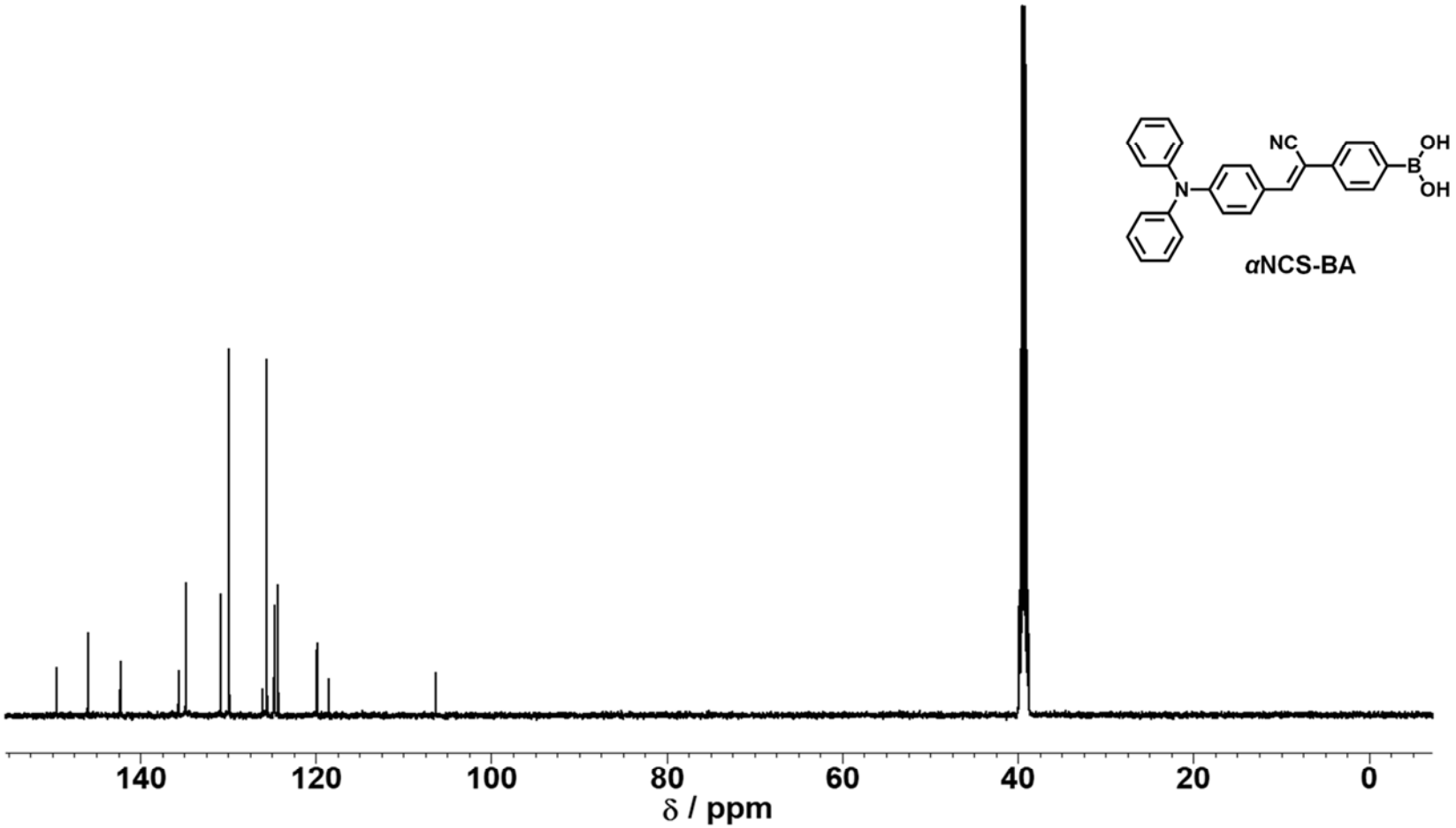

Fig. S23. ^{13}C NMR spectrum (126 MHz) of ***α*NCS-BA** in DMSO-d_6.

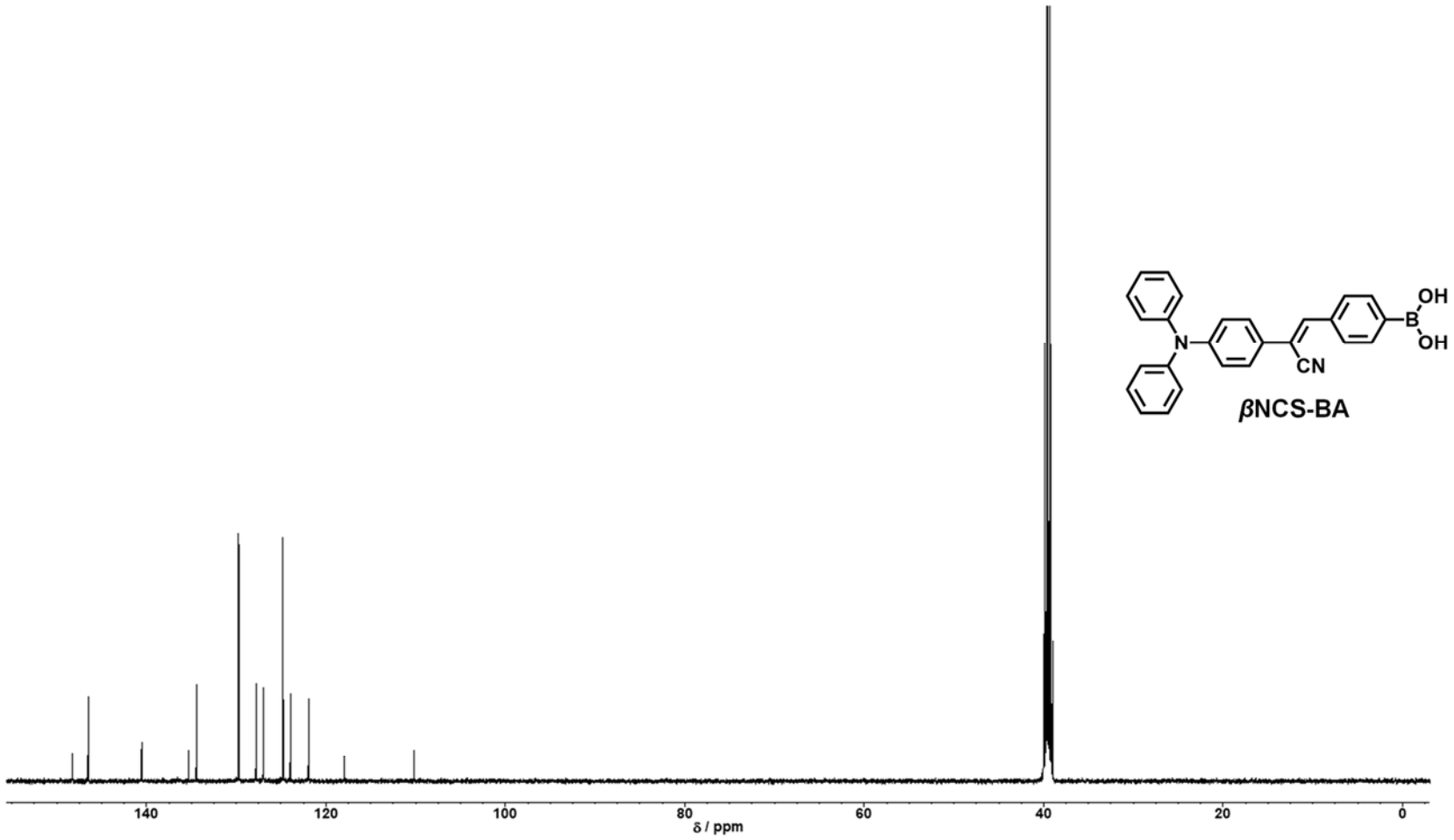

Fig. S24. ^{13}C NMR spectrum (126 MHz) of ***β*NCS-BA** in DMSO-d_6.

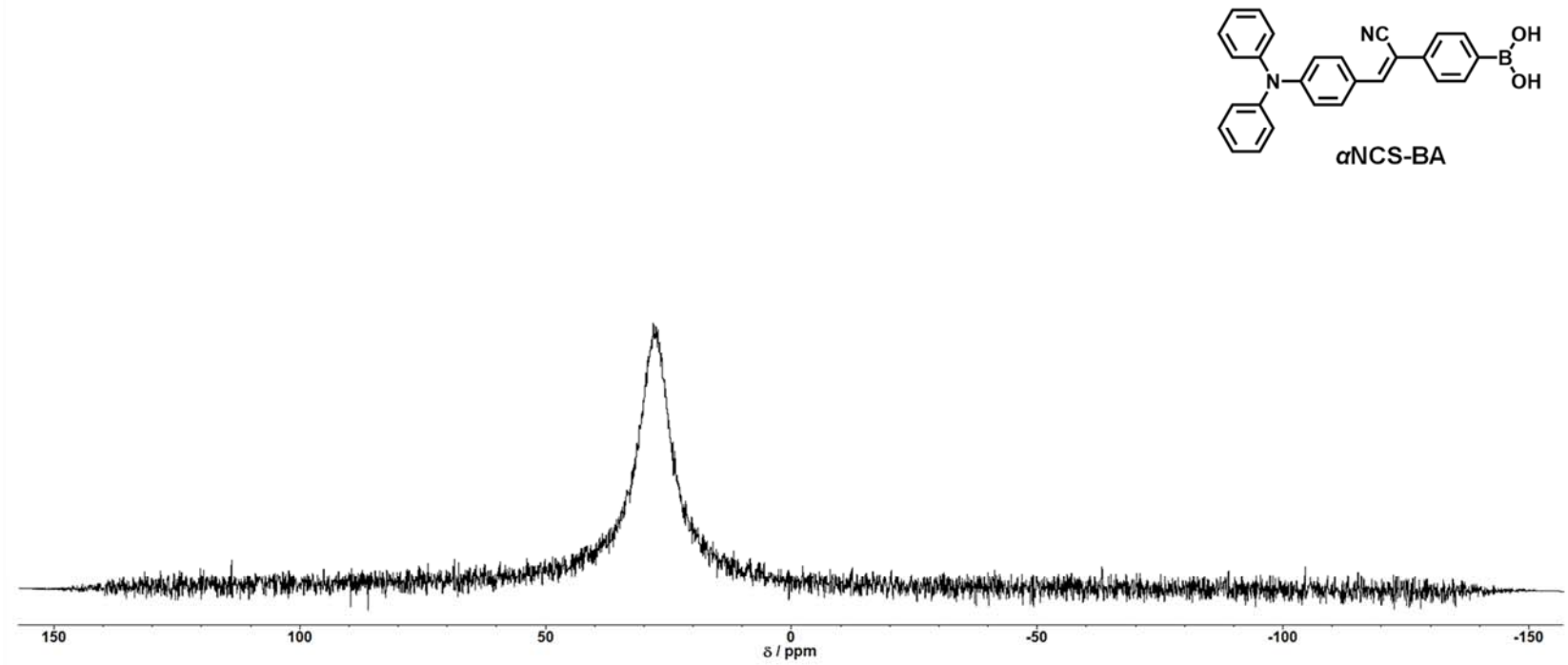

Fig. S25. ^{11}B NMR spectrum (128 MHz) of ***α*NCS-BA** in THF-d_8.

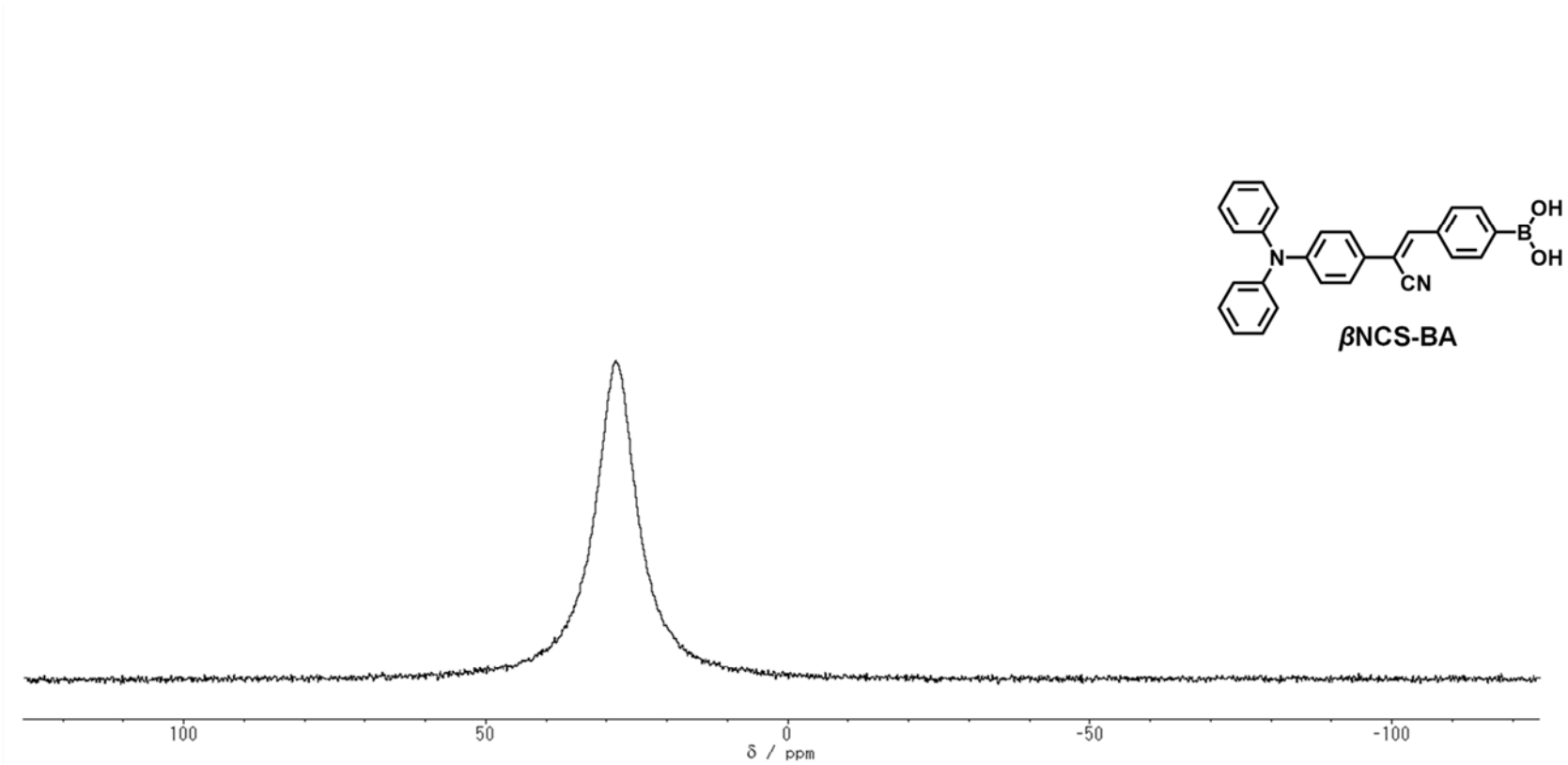

Fig. S26. ^{11}B NMR spectrum (128 MHz) of ***β*NCS-BA** in THF-d_8.

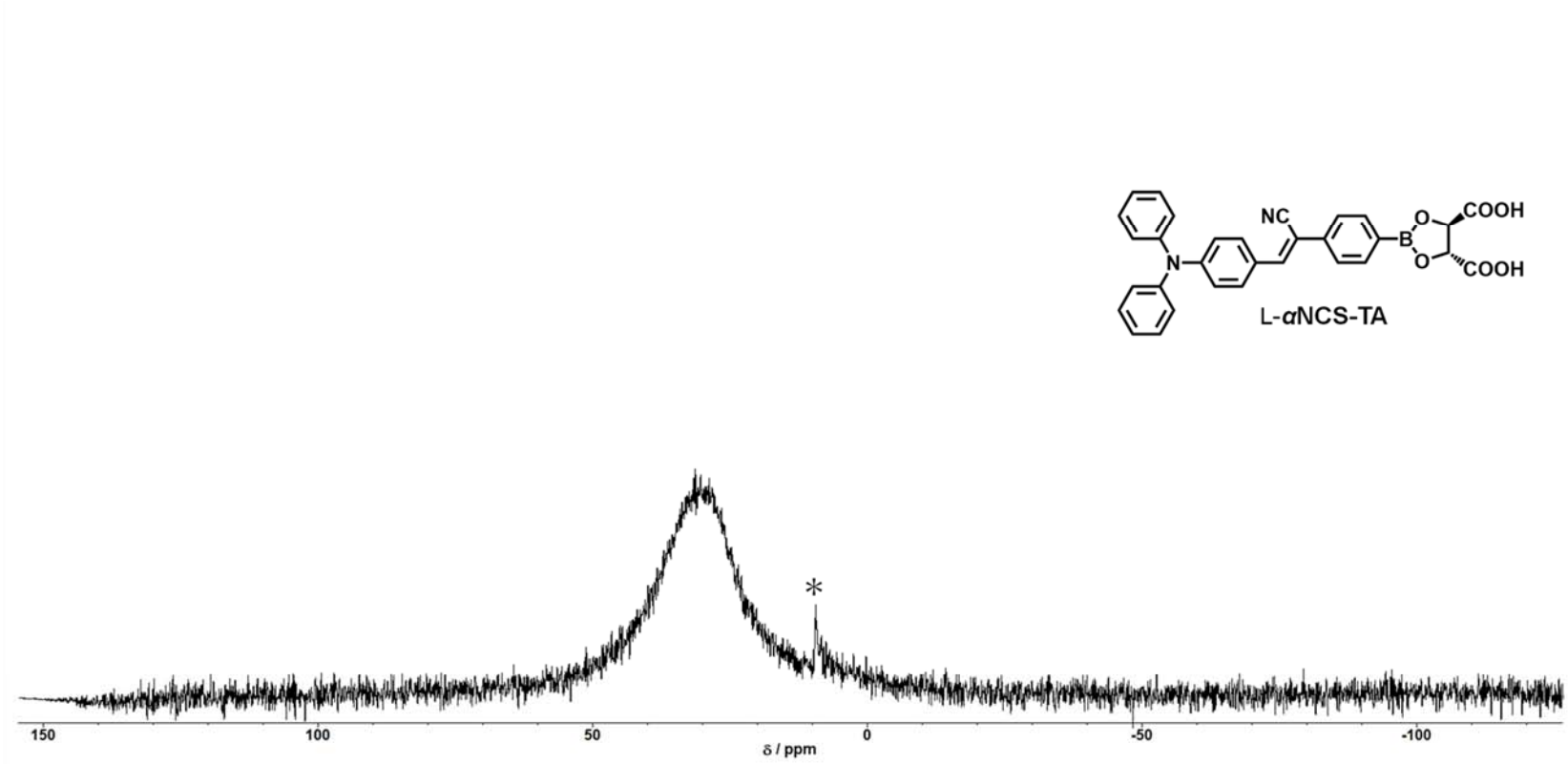

Fig. S27. ^{11}B NMR spectrum (128 MHz) of L-***α*NCS-TA in THF-d_8. The peak (*) at 9.39 ppm may be due to unidentified impurity.

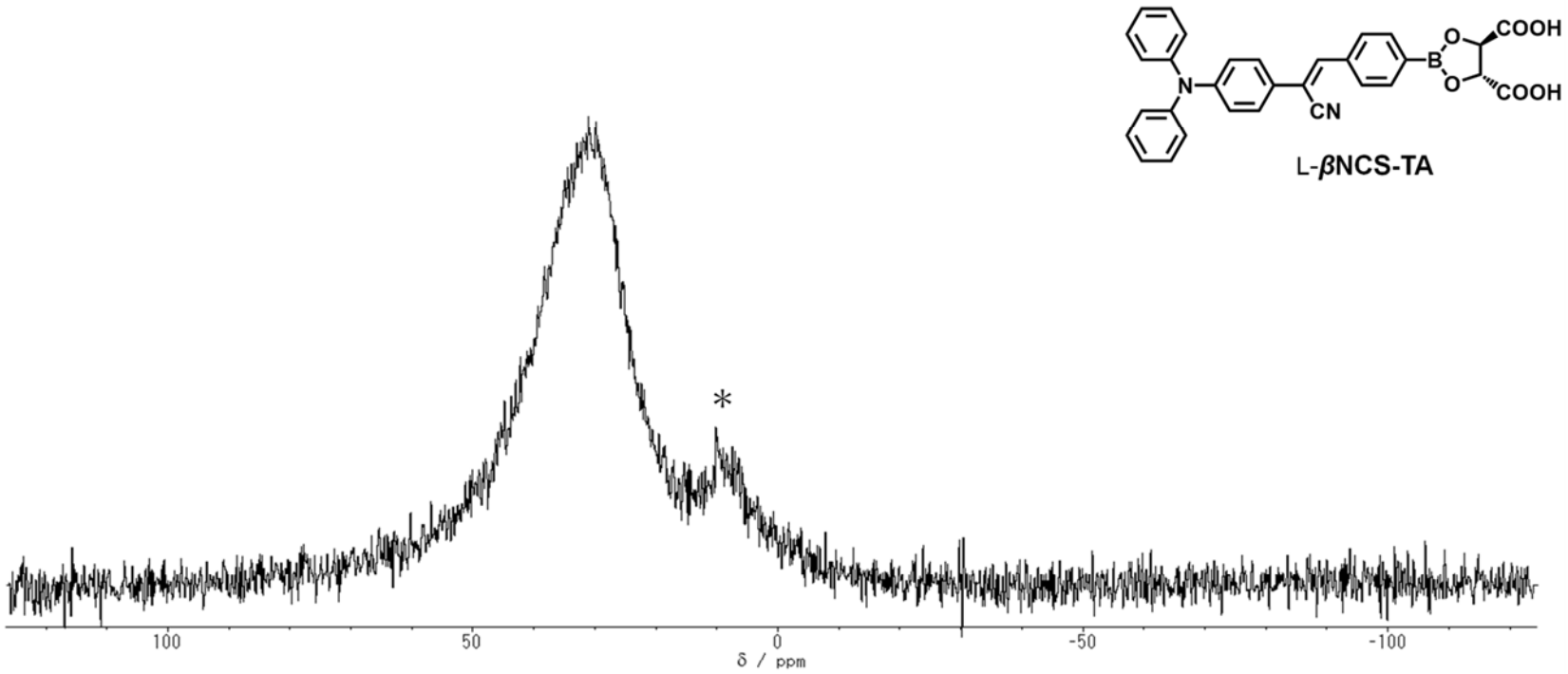

Fig. S28. ^{11}B NMR spectrum (128 MHz) of L-***β*NCS-TA in THF-d_8. The peak (*) at 10.17 ppm may be due to unidentified impurity.

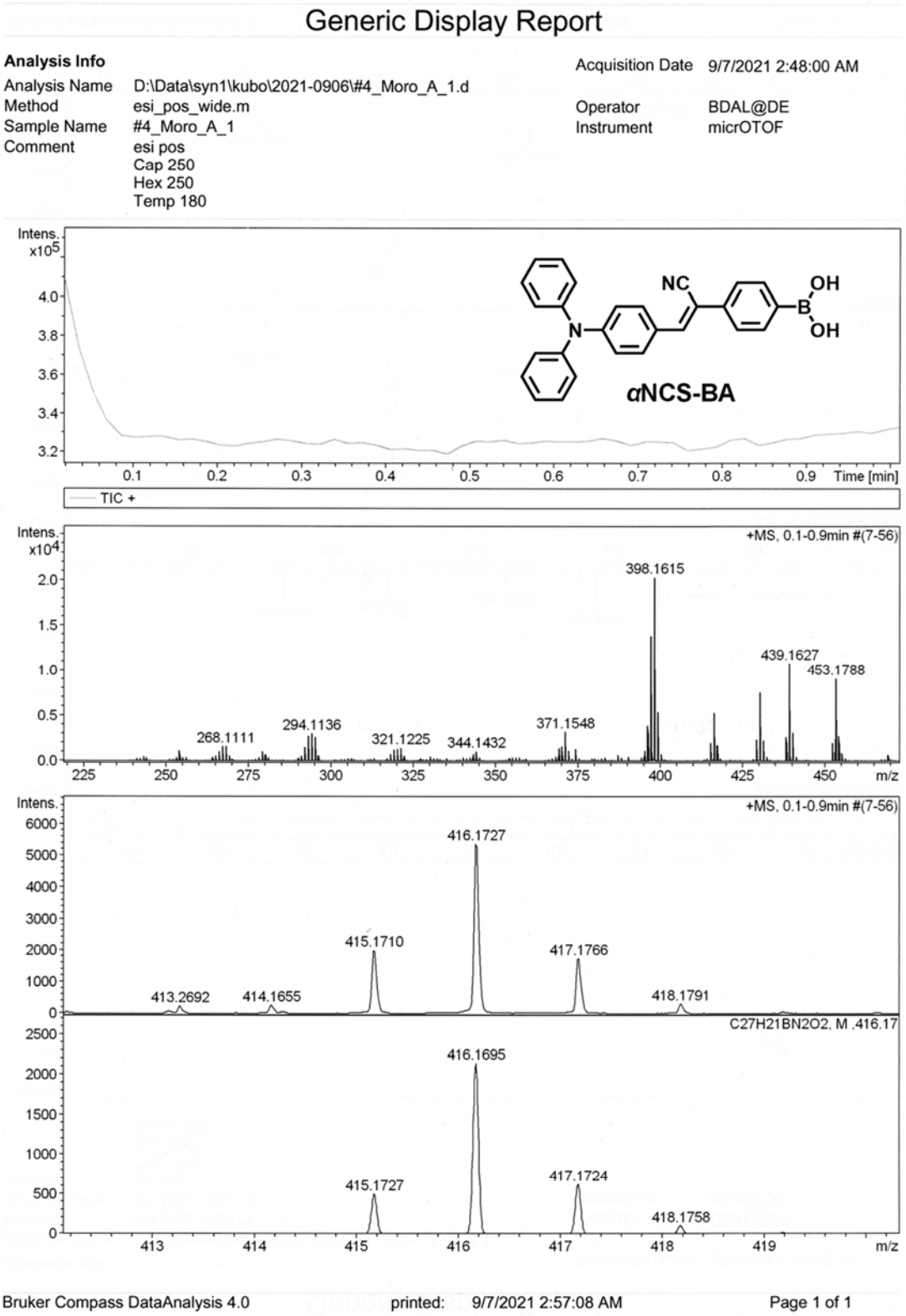

Fig. S29. High resolution of ESI mass spectrum (positive mode) of ***α*NCS-BA**.

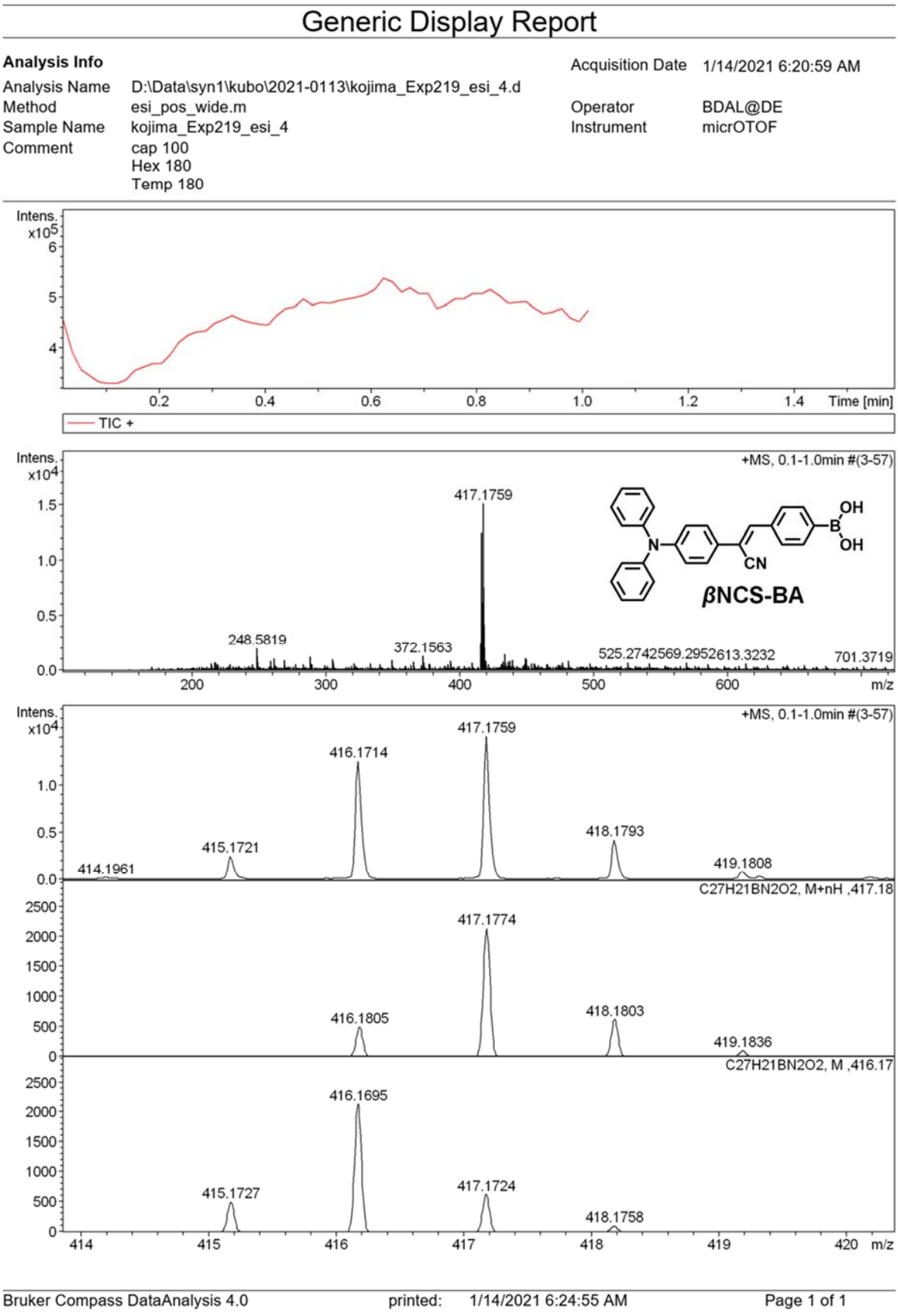

Fig. S30. High resolution of ESI mass spectrum (positive mode) of ***β*NCS-BA**.

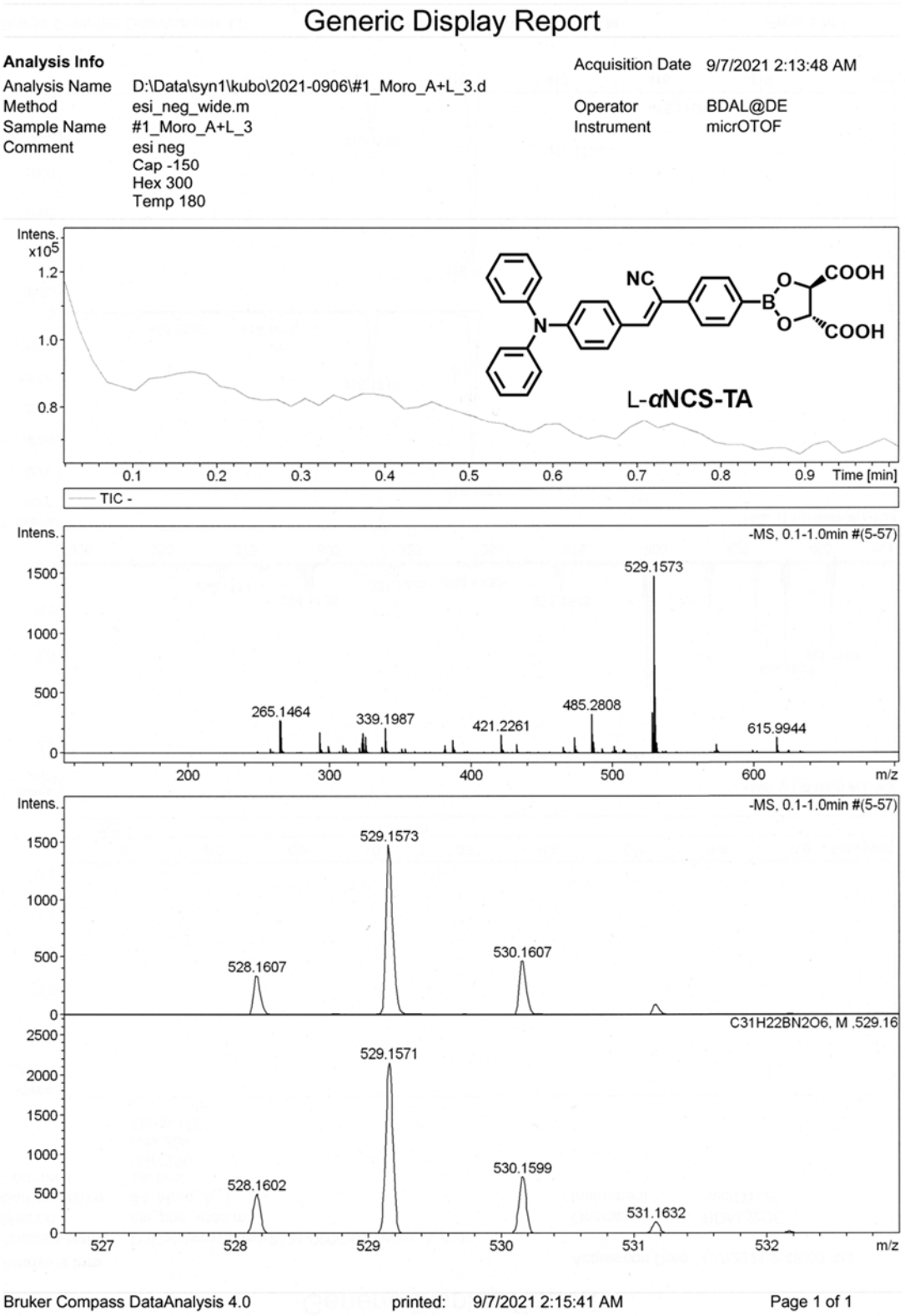

Fig. S31. High resolution of ESI mass spectrum (negative mode) of L-***α*NCS-TA.

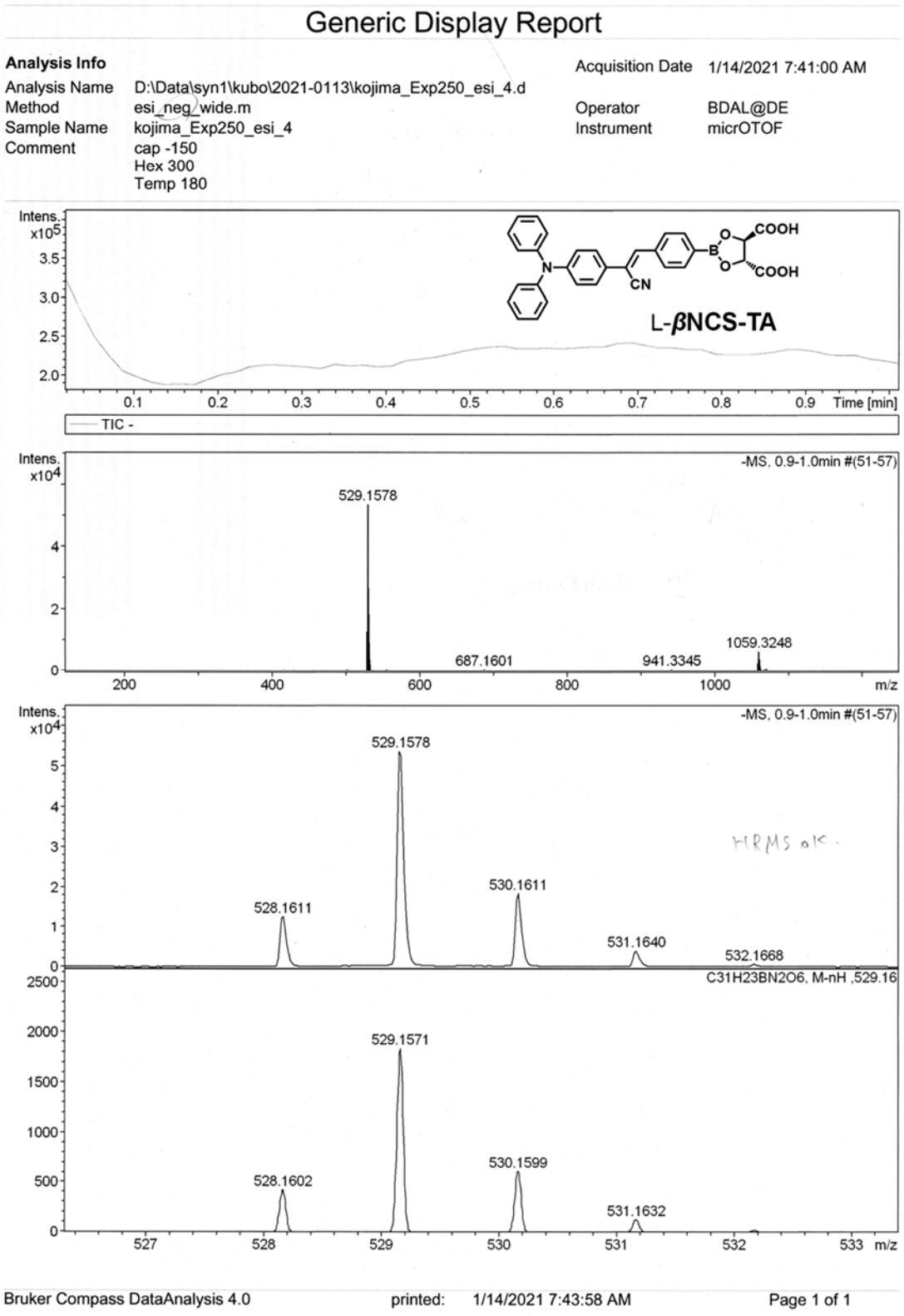

Fig. S32. High resolution of ESI mass spectrum (negative mode) of L-***β*NCS-TA.

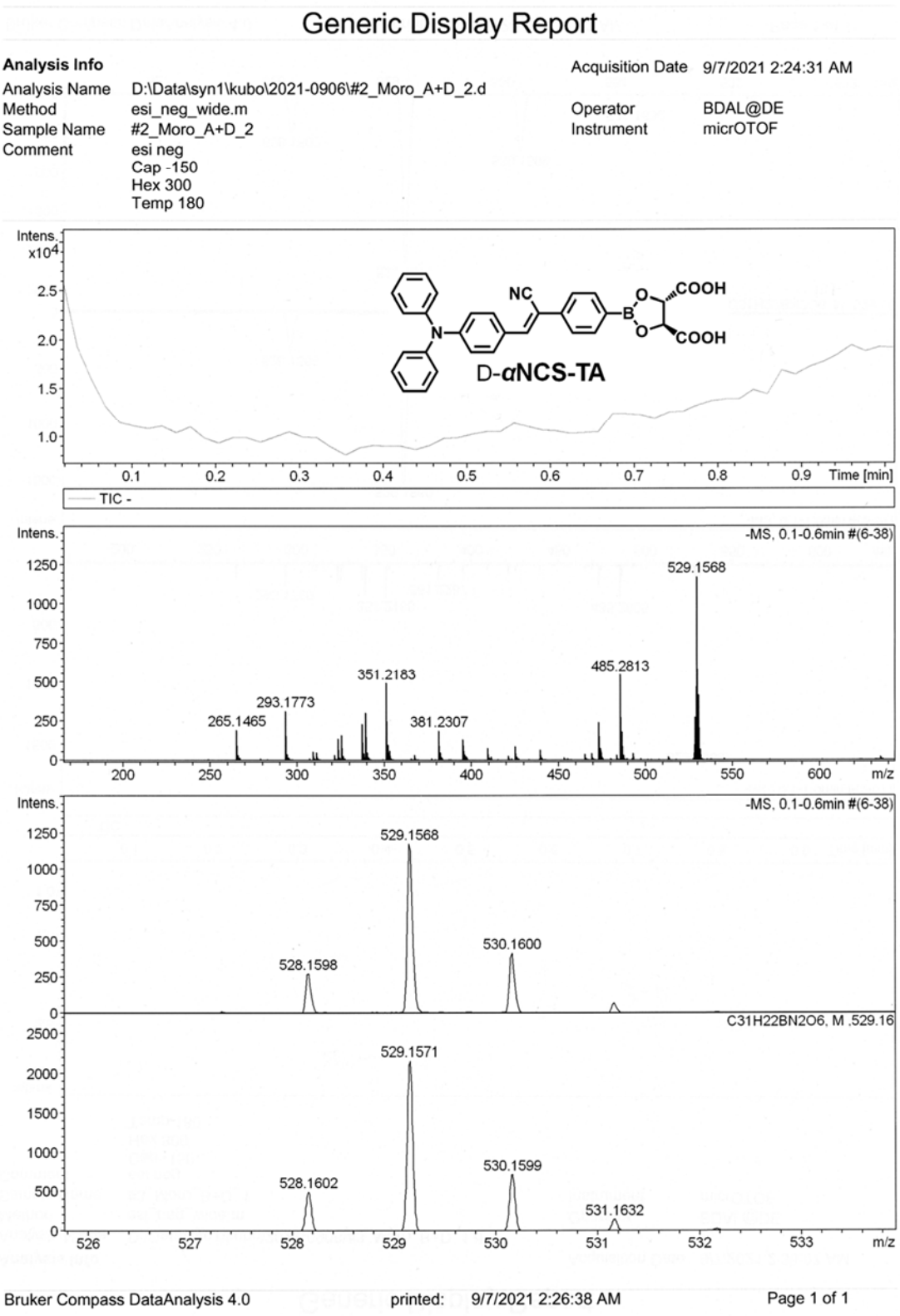

Fig. S33. High resolution of ESI mass spectrum (negative mode) of D-***α*NCS-TA.

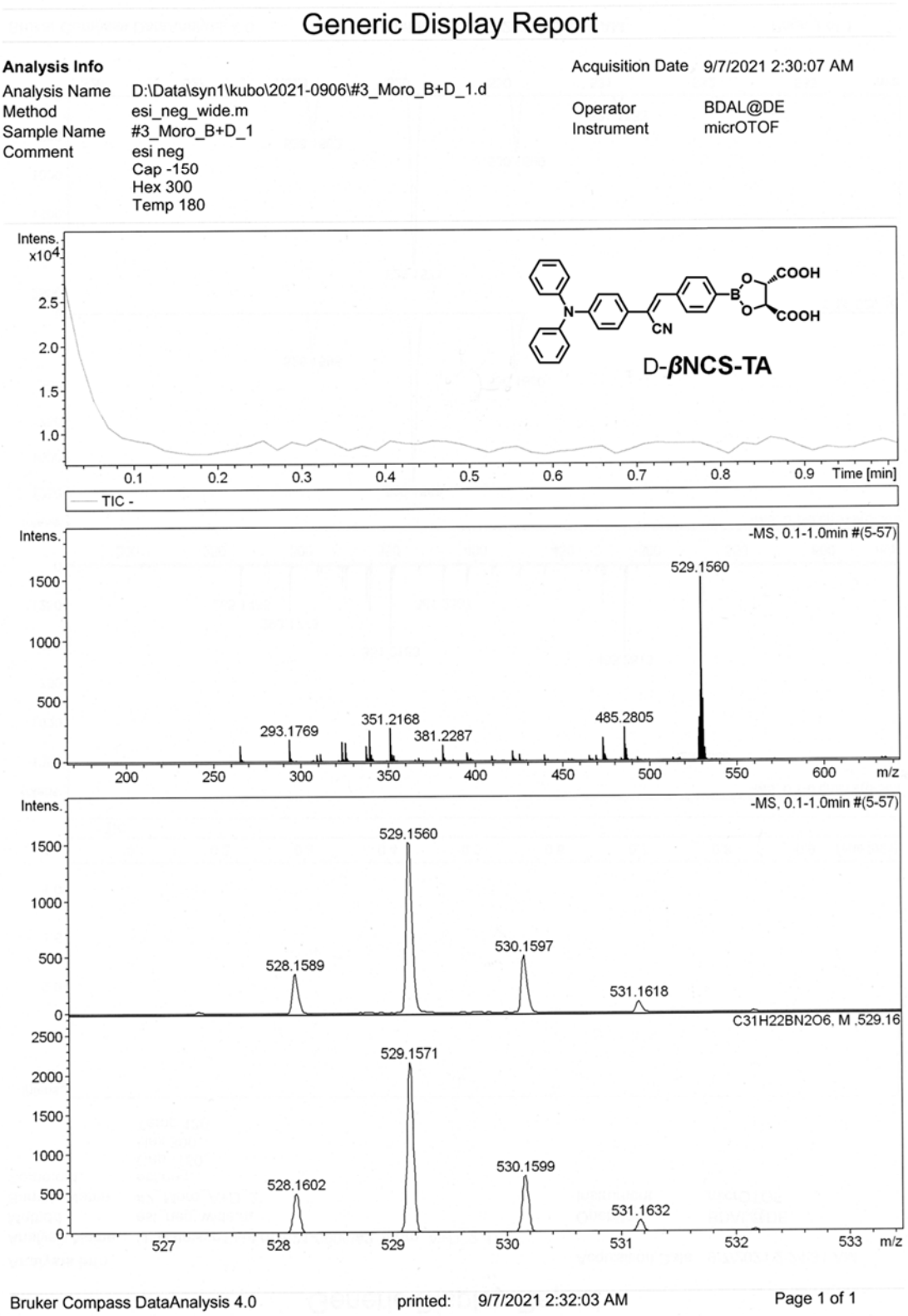

Fig. S34. High resolution of ESI mass spectrum (negative mode) of D-***β*NCS-TA.

Single Crystal Structure Report for *β*NCS-BA (CCDC No. 2109188)

A specimen of $C_{27}H_{21}BN_2O_2$, approximate dimensions 0.200 mm x 0.200 mm x 0.200 mm, was used for the X-ray crystallographic analysis. The X-ray intensity data were measured (λ = 1.54178 Å).

The total exposure time was 6.65 hours. The frames were integrated with the Bruker SAINT software package using a narrow-frame algorithm. The integration of the data using a triclinic unit cell yielded a total of 10082 reflections to a maximum θ angle of 72.39° (0.81 Å resolution), of which 4160 were independent (average redundancy 2.424, completeness = 96.2%, R_{int} = 2.50%, R_{sig} = 2.90%) and 3747 (90.07%) were greater than $2\sigma(F^2)$. The final cell constants of a = 7.6398(2) Å, b = 9.7054(3) Å, c = 15.9804(5) Å, α = 94.283(2)°, β = 100.6460(10)°, γ = 108.9560(10)°, volume = 1089.73(6) $Å^3$, are based upon the refinement of the XYZ-centroids of 7918 reflections above 20 σ(I) with 5.688° < 2θ < 144.8°. Data were corrected for absorption effects using the Multi-Scan method (SADABS). The ratio of minimum to maximum apparent transmission was 0.890. The calculated minimum and maximum transmission coefficients (based on crystal size) are 0.8840 and 0.8840.

The structure was solved and refined using the Bruker SHELXTL Software Package, using the space group P -1, with Z = 2 for the formula unit, $C_{27}H_{21}BN_2O_2$. The final anisotropic full-matrix least-squares refinement on F^2 with 293variables converged at R1 = 4.14%, for the observed data and wR2 = 11.10% for all data. The goodness-of-fit was 1.017. The largest peak in the final difference electron density synthesis was 0.302 $e^-/Å^3$ and the largest hole was-0.312 $e^-/Å^3$ with an RMS deviation of 0.037 $e^-/Å^3$. On the basis of the final model, the calculated density was 1.269 g/cm^3 and F(000), 436 e^-.

Table S4. Sample and crystal data for ***β*NCS-BA**.

Identification code	*β*NCSBA	
Chemical formula	C27H21BN2O2	
Formula weight	416.27 g/mol	
Temperature	100(2) K	
Wavelength	1.54178 Å	
Crystal size	0.200 x 0.200 x 0.200 mm	
Crystal system	triclinic	
Space group	P -1	
Unit cell dimensions	a = 7.6398(2) Å	α = 94.283(2)°
	b = 9.7054(3) Å	β = 100.6460(10)°
	c = 15.9804(5) Å	γ = 108.9560(10)°
Volume	1089.73(6) $Å^3$	
Z	2	
Density (calculated)	1.269 g/cm^3	
Absorption coefficient	0.631 mm^{-1}	
F(000)	436	

Table S5. Data collection and structure refinement for ***β*NCS-BA**.

Theta range for data collection	2.84 to 72.39°	
Index ranges	-9<=h<=9, -11<=k<=11, -19<=l<=19	
Reflections collected	10082	
Independent reflections	4160 [R(int) = 0.0250]	
Coverage of independent reflections	96.20%	
Absorption correction	Multi-Scan	
Max. and min. transmission	0.8840 and 0.8840	
Structure solution technique	direct methods	
Structure solution program	SHELXT 2014/5 (Sheldrick, 2014)	
Refinement method	Full-matrix least-squares on F^2	
Refinement program	SHELXL-2018/3 (Sheldrick, 2018)	
Function minimized	$\Sigma\ w(Fo^2 - Fc^2)^2$	
Data / restraints / parameters	4160 / 0 / 293	
Goodness-of-fit on F2	1.017	
Final R indices	3747 data; I>2σ(I)	R1 = 0.0414, wR2 = 0.1075
	all data	R1 = 0.0455, wR2 = 0.1110
Weighting scheme	$w=1/[\sigma^2(Fo^2)+(0.0535P)^2+0.4189P]$	
	where $P=(Fo^2+2Fc^2)/3$	
Largest diff. peak and hole	0.302 and -0.312 $eÅ^{-3}$	
R.M.S. deviation from mean	0.037 $eÅ^{-3}$	

Table S6. Atomic coordinates and equivalent isotropic atomic displacement parameters (Å^2) for ***β*NCS-BA**.

	x/a	y/b	z/c	U(eq)
B1	0.7004(2)	0.90972(16)	0.05063(9)	0.0255(3)
O1	0.71803(14)	0.05480(10)	0.06217(7)	0.0314(2)
C1	0.86741(19)	0.85057(14)	0.08205(8)	0.0256(3)
N1	0.04402(17)	0.30474(13)	0.11094(8)	0.0333(3)
O2	0.53021(14)	0.80993(10)	0.01017(7)	0.0325(2)
C2	0.0573(2)	0.94121(14)	0.10933(9)	0.0294(3)
N2	0.98641(16)	0.44726(12)	0.34489(8)	0.0309(3)
C5	0.9679(2)	0.64111(15)	0.10824(9)	0.0296(3)
C4	0.15816(19)	0.73287(14)	0.13488(8)	0.0256(3)
C3	0.1995(2)	0.88432(15)	0.13502(9)	0.0302(3)
C6	0.8271(2)	0.69939(15)	0.08222(9)	0.0291(3)
C7	0.31702(19)	0.68323(14)	0.16647(8)	0.0258(3)
C8	0.32407(18)	0.54680(14)	0.17064(8)	0.0247(3)
C9	0.16413(19)	0.41523(14)	0.13547(9)	0.0264(3)
C10	0.49548(18)	0.51920(14)	0.21557(9)	0.0247(3)
C11	0.61180(18)	0.61152(13)	0.29022(9)	0.0243(3)
C12	0.77165(18)	0.58784(14)	0.33322(9)	0.0253(3)
C13	0.82127(18)	0.47005(14)	0.30212(9)	0.0272(3)
C14	0.70313(19)	0.37538(14)	0.22847(10)	0.0315(3)
C15	0.54238(19)	0.39903(14)	0.18645(10)	0.0300(3)
C16	0.9907(2)	0.30110(15)	0.34384(11)	0.0332(3)
C17	0.8459(3)	0.1911(2)	0.3651(2)	0.0772(8)
C18	0.8515(3)	0.0493(2)	0.3624(3)	0.1024(12)
C19	0.0006(3)	0.01711(18)	0.33979(18)	0.0670(7)
C20	0.1467(2)	0.12738(16)	0.32048(10)	0.0340(3)
C21	0.14187(18)	0.26868(14)	0.32204(8)	0.0248(3)
C22	0.14908(19)	0.56617(14)	0.38919(9)	0.0261(3)
C23	0.20121(18)	0.70181(14)	0.35903(8)	0.0240(3)
C24	0.36227(19)	0.81639(15)	0.40300(9)	0.0282(3)
C25	0.4769(2)	0.79764(17)	0.47643(10)	0.0388(4)
C26	0.4250(3)	0.66268(18)	0.50576(10)	0.0477(5)
C27	0.2630(3)	0.54858(17)	0.46347(9)	0.0391(4)

U(eq) is defined as one third of the trace of the orthogonalized Uij tensor.

Table S7. Bond lengths (Å) for ***β*NCS-BA**.

atom	distance	atom	distance
B1-O2	1.3506(18)	B1-O1	1.3652(17)
B1-C1	1.579(2)	O1-H1	0.83(2)
C1-C2	1.3956(19)	C1-C6	1.3982(18)
N1-C9	1.1449(18)	O2-H2A	0.85(2)
C2-C3	1.383(2)	C2-H2	0.95
N2-C13	1.4117(17)	N2-C22	1.4137(18)
N2-C16	1.4286(16)	C5-C6	1.3839(19)
C5-C4	1.4004(19)	C5-H5	0.95
C4-C3	1.3993(18)	C4-C7	1.4661(18)
C3-H3	0.95	C6-H6	0.95
C7-C8	1.3487(18)	C7-H7	0.95
C8-C9	1.4369(18)	C8-C10	1.4871(18)
C10-C11	1.3954(19)	C10-C15	1.3989(18)
C11-C12	1.3828(18)	C11-H11	0.95
C12-C13	1.4014(18)	C12-H12	0.95
C13-C14	1.397(2)	C14-C15	1.383(2)
C14-H14	0.95	C15-H15	0.95
C16-C17	1.380(2)	C16-C21	1.3863(18)
C17-C18	1.388(2)	C17-H17	0.95
C18-C19	1.376(3)	C18-H18	0.95
C19-C20	1.373(2)	C19-H19	0.95
C20-C21	1.3821(19)	C20-H20	0.95
C21-H21	0.95	C22-C27	1.393(2)
C22-C23	1.3961(18)	C23-C24	1.3854(19)
C23-H23	0.95	C24-C25	1.390(2)
C24-H24	0.95	C25-C26	1.384(3)
C25-H25	0.95	C26-C27	1.380(2)
C26-H26	0.95	C27-H27	0.95

Table S8. Bond angles (°) for ***β*NCS-BA**.

atom	angle	atom	angle
O2-B1-O1	118.48(12)	O2-B1-C1	117.58(12)
O1-B1-C1	123.94(12)	B1-O1-H1	109.5
C2-C1-C6	116.98(12)	C2-C1-B1	123.59(12)
C6-C1-B1	119.42(12)	B1-O2-H2A	109.5
C3-C2-C1	121.64(12)	C3-C2-H2	119.2
C1-C2-H2	119.2	C13-N2-C22	121.53(10)
C13-N2-C16	119.71(12)	C22-N2-C16	118.76(11)
C6-C5-C4	120.62(12)	C6-C5-H5	119.7
C4-C5-H5	119.7	C3-C4-C5	117.71(12)
C3-C4-C7	117.24(12)	C5-C4-C7	124.99(12)
C2-C3-C4	121.07(13)	C2-C3-H3	119.5
C4-C3-H3	119.5	C5-C6-C1	121.97(13)
C5-C6-H6	119	C1-C6-H6	119
C8-C7-C4	131.10(12)	C8-C7-H7	114.5
C4-C7-H7	114.5	C7-C8-C9	123.01(12)
C7-C8-C10	122.93(12)	C9-C8-C10	114.01(11)
N1-C9-C8	174.85(14)	C11-C10-C15	118.01(12)
C11-C10-C8	120.26(11)	C15-C10-C8	121.70(12)
C12-C11-C10	121.30(12)	C12-C11-H11	119.3
C10-C11-H11	119.3	C11-C12-C13	120.38(13)
C11-C12-H12	119.8	C13-C12-H12	119.8
C14-C13-C12	118.56(12)	C14-C13-N2	120.89(12)
C12-C13-N2	120.54(13)	C15-C14-C13	120.60(12)
C15-C14-H14	119.7	C13-C14-H14	119.7
C14-C15-C10	121.08(13)	C14-C15-H15	119.5
C10-C15-H15	119.5	C17-C16-C21	119.28(13)
C17-C16-N2	120.59(13)	C21-C16-N2	120.13(12)
C16-C17-C18	119.64(16)	C16-C17-H17	120.2
C18-C17-H17	120.2	C19-C18-C17	120.96(17)
C19-C18-H18	119.5	C17-C18-H18	119.5
C20-C19-C18	119.34(15)	C20-C19-H19	120.3
C18-C19-H19	120.3	C19-C20-C21	120.29(14)
C19-C20-H20	119.9	C21-C20-H20	119.9
C20-C21-C16	120.48(13)	C20-C21-H21	119.8
C16-C21-H21	119.8	C27-C22-C23	118.67(13)
C27-C22-N2	120.10(12)	C23-C22-N2	121.21(12)
C24-C23-C22	120.24(12)	C24-C23-H23	119.9
C22-C23-H23	119.9	C23-C24-C25	120.86(13)
C23-C24-H24	119.6	C25-C24-H24	119.6
C26-C25-C24	118.62(14)	C26-C25-H25	120.7
C24-C25-H25	120.7	C27-C26-C25	121.07(14)
C27-C26-H26	119.5	C25-C26-H26	119.5
C26-C27-C22	120.53(14)	C26-C27-H27	119.7
C22-C27-H27	119.7		

Table S9. Anisotropic atomic displacement parameters (Å^2) for ***β*NCS-BA**.

atom	U11	U22	U33	U23	U13	U12
B1	0.0322(8)	0.0217(7)	0.0226(7)	0.0029(5)	0.0039(6)	0.0105(6)
O1	0.0285(5)	0.0222(5)	0.0396(6)	-0.0009(4)	-0.0035(4)	0.0109(4)
C1	0.0330(7)	0.0239(6)	0.0210(6)	0.0026(5)	0.0037(5)	0.0129(5)
N1	0.0344(6)	0.0228(6)	0.0413(7)	0.0015(5)	0.0012(5)	0.0126(5)
O2	0.0314(5)	0.0217(5)	0.0417(6)	0.0035(4)	-0.0020(4)	0.0115(4)
C2	0.0351(7)	0.0185(6)	0.0336(7)	0.0017(5)	0.0020(6)	0.0114(5)
N2	0.0294(6)	0.0203(5)	0.0507(7)	0.0114(5)	0.0128(5)	0.0153(5)
C5	0.0344(7)	0.0209(6)	0.0349(7)	0.0088(5)	0.0054(6)	0.0115(5)
C4	0.0322(7)	0.0233(6)	0.0238(6)	0.0049(5)	0.0062(5)	0.0126(5)
C3	0.0302(7)	0.0232(7)	0.0348(7)	0.0015(5)	0.0021(6)	0.0094(5)
C6	0.0300(7)	0.0238(7)	0.0317(7)	0.0062(5)	0.0028(5)	0.0088(5)
C7	0.0280(6)	0.0224(6)	0.0286(6)	0.0054(5)	0.0076(5)	0.0097(5)
C8	0.0277(6)	0.0213(6)	0.0279(6)	0.0046(5)	0.0103(5)	0.0097(5)
C9	0.0321(7)	0.0232(7)	0.0290(7)	0.0050(5)	0.0079(5)	0.0153(6)
C10	0.0242(6)	0.0186(6)	0.0355(7)	0.0076(5)	0.0138(5)	0.0083(5)
C11	0.0278(6)	0.0186(6)	0.0338(7)	0.0080(5)	0.0141(5)	0.0126(5)
C12	0.0274(6)	0.0202(6)	0.0337(7)	0.0080(5)	0.0119(5)	0.0115(5)
C13	0.0258(6)	0.0190(6)	0.0440(8)	0.0118(5)	0.0162(6)	0.0112(5)
C14	0.0281(7)	0.0166(6)	0.0549(9)	0.0033(6)	0.0187(6)	0.0099(5)
C15	0.0254(6)	0.0191(6)	0.0463(8)	0.0011(6)	0.0138(6)	0.0065(5)
C16	0.0303(7)	0.0207(7)	0.0577(9)	0.0145(6)	0.0170(6)	0.0152(6)
C17	0.0532(11)	0.0419(10)	0.177(3)	0.0588(14)	0.0726(15)	0.0349(9)
C18	0.0554(12)	0.0394(11)	0.250(4)	0.0734(17)	0.0802(18)	0.0290(10)
C19	0.0419(9)	0.0216(8)	0.147(2)	0.0239(10)	0.0239(11)	0.0193(7)
C20	0.0278(7)	0.0283(7)	0.0480(8)	-0.0005(6)	0.0019(6)	0.0173(6)
C21	0.0221(6)	0.0236(6)	0.0294(7)	0.0041(5)	0.0029(5)	0.0103(5)
C22	0.0329(7)	0.0231(6)	0.0308(7)	0.0053(5)	0.0118(5)	0.0182(5)
C23	0.0246(6)	0.0257(6)	0.0286(6)	0.0071(5)	0.0080(5)	0.0159(5)
C24	0.0293(7)	0.0252(6)	0.0346(7)	0.0022(5)	0.0084(5)	0.0152(5)
C25	0.0456(9)	0.0346(8)	0.0361(8)	-0.0105(6)	-0.0042(6)	0.0242(7)
C26	0.0783(12)	0.0413(9)	0.0274(7)	-0.0070(7)	-0.0117(8)	0.0411(9)
C27	0.0707(11)	0.0301(7)	0.0264(7)	0.0059(6)	0.0084(7)	0.0316(8)

The anisotropic atomic displacement factor exponent takes the form: $-2\pi^2[\ h^2\ a^{*2}\ U_{11} + ... + 2\ h\ k\ a^*\ b^*\ U_{12}\ ]$

Table S10. Hydrogen atomic coordinates and isotropic atomic displacement parameters (Å^2) for ***β*NCS-BA**.

atom	x/a	y/b	z/c	U(eq)
H1	-0.168(3)	1.1063(13)	0.0785(13)	0.047
H2A	-0.547(2)	0.8543(12)	-0.0063(12)	0.049
H2	0.0896	1.0445	0.1103	0.035
H5	-0.0649	0.5379	0.108	0.036
H3	0.3274	0.9491	0.153	0.036
H6	-0.3008	0.6348	0.0639	0.035
H7	0.4353	0.7605	0.1876	0.031
H11	0.5806	0.6922	0.3119	0.029
H12	0.8483	0.6518	0.3841	0.03
H14	0.7335	0.294	0.207	0.038
H15	0.4625	0.3326	0.137	0.036
H17	0.743	0.2123	0.3815	0.093
H18	0.7509	-0.0265	0.3763	0.123
H19	1.0026	-0.0805	0.3376	0.08
H20	1.2514	0.1065	0.306	0.041
H21	1.2429	0.3441	0.3081	0.03
H23	1.126	0.7156	0.3082	0.029
H24	1.3948	0.909	0.3827	0.034
H25	1.5885	0.8758	0.5059	0.047
H26	1.5022	0.6484	0.5558	0.057
H27	1.2288	0.4573	0.4852	0.047

Table S11. Measurement information of entire data for LDA input.

Host	Guest	f_{EtOH} / %	T / ℃	[Host] / mM	Host:Guest / *eq*	λ_{ex} / nm
L-***α*NCS-TA**	(1*R*,2*R*)-**CHDA**	20	25	0.75	1	365
L-***α*NCS-TA**	(1*R*,2*R*)-**CHDA**	40	25	0.75	1	365
L-***α*NCS-TA**	(1*R*,2*R*)-**CHDA**	60	25	0.75	1	365
L-***α*NCS-TA**	(1*R*,2*R*)-**CHDA**	80	25	0.75	1	365
L-***α*NCS-TA**	(1*R*,2*R*)-**CHDA**	90	25	0.75	1	365
L-***α*NCS-TA**	(1*R*,2*R*)-**CHDA**	10	25	0.75	1	365
L-***α*NCS-TA**	(1*R*,2*R*)-**CHDA**	20	25	0.75	1	365
L-***α*NCS-TA**	(1*R*,2*R*)-**CHDA**	30	25	0.75	1	365
L-***α*NCS-TA**	(1*R*,2*R*)-**CHDA**	40	25	0.75	1	365
L-***α*NCS-TA**	(1*R*,2*R*)-**CHDA**	50	25	0.75	1	365
L-***α*NCS-TA**	(1*R*,2*R*)-**CHDA**	60	25	0.75	1	365
L-***α*NCS-TA**	(1*R*,2*R*)-**CHDA**	70	25	0.75	1	365
L-***α*NCS-TA**	(1*R*,2*R*)-**CHDA**	75	25	0.75	1	365
L-***α*NCS-TA**	(1*R*,2*R*)-**CHDA**	80	25	0.75	1	365
L-***α*NCS-TA**	(1*R*,2*R*)-**CHDA**	90	25	0.75	1	365
L-***α*NCS-TA**	(1*R*,2*R*)-**CHDA**	90	25	0.75	1	365
L-***α*NCS-TA**	(1*R*,2*R*)-**CHDA**	75	25	0.75	1	365
L-***α*NCS-TA**	(1*R*,2*R*)-**CHDA**	75	25	0.75	1	365
L-***α*NCS-TA**	(1*R*,2*R*)-**CHDA**	90	25	0.75	1	330
L-***α*NCS-TA**	(1*R*,2*R*)-**CHDA**	90	25	0.75	1	340
L-***α*NCS-TA**	(1*R*,2*R*)-**CHDA**	90	25	0.75	1	350
L-***α*NCS-TA**	(1*R*,2*R*)-**CHDA**	90	25	0.75	1	360
L-***α*NCS-TA**	(1*R*,2*R*)-**CHDA**	90	25	0.75	1	370
L-***α*NCS-TA**	(1*R*,2*R*)-**CHDA**	90	25	0.75	1	380
L-***α*NCS-TA**	(1*R*,2*R*)-**CHDA**	90	25	0.75	1	390
L-***α*NCS-TA**	(1*R*,2*R*)-**CHDA**	90	25	0.75	1	400
L-***α*NCS-TA**	(1*R*,2*R*)-**CHDA**	90	25	0.75	1	410
L-***α*NCS-TA**	(1*R*,2*R*)-**CHDA**	90	25	0.75	1	420
L-***α*NCS-TA**	(1*R*,2*R*)-**CHDA**	90	25	0.75	1	430
L-***α*NCS-TA**	(1*R*,2*R*)-**CHDA**	90	25	0.75	1	440
L-***α*NCS-TA**	(1*S*,2*S*)-**CHDA**	20	25	0.75	1	365
L-***α*NCS-TA**	(1*S*,2*S*)-**CHDA**	40	25	0.75	1	365
L-***α*NCS-TA**	(1*S*,2*S*)-**CHDA**	60	25	0.75	1	365
L-***α*NCS-TA**	(1*S*,2*S*)-**CHDA**	80	25	0.75	1	365
L-***α*NCS-TA**	(1*S*,2*S*)-**CHDA**	90	25	0.75	1	365
L-***α*NCS-TA**	(1*S*,2*S*)-**CHDA**	10	25	0.75	1	365
L-***α*NCS-TA**	(1*S*,2*S*)-**CHDA**	20	25	0.75	1	365
L-***α*NCS-TA**	(1*S*,2*S*)-**CHDA**	30	25	0.75	1	365
L-***α*NCS-TA**	(1*S*,2*S*)-**CHDA**	40	25	0.75	1	365
L-***α*NCS-TA**	(1*S*,2*S*)-**CHDA**	50	25	0.75	1	365
L-***α*NCS-TA**	(1*S*,2*S*)-**CHDA**	60	25	0.75	1	365
L-***α*NCS-TA**	(1*S*,2*S*)-**CHDA**	70	25	0.75	1	365
L-***α*NCS-TA**	(1*S*,2*S*)-**CHDA**	75	25	0.75	1	365
L-***α*NCS-TA**	(1*S*,2*S*)-**CHDA**	80	25	0.75	1	365

L-***α*NCS-TA**	(1*S*,2*S*)-**CHDA**	90	25	0.75	1	365
L-***α*NCS-TA**	(1*S*,2*S*)-**CHDA**	90	25	0.75	1	365
L-***α*NCS-TA**	(1*S*,2*S*)-**CHDA**	75	25	0.75	1	365
L-***α*NCS-TA**	(1*S*,2*S*)-**CHDA**	75	25	0.75	1	365
L-***α*NCS-TA**	(1*S*,2*S*)-**CHDA**	90	25	0.75	1	330
L-***α*NCS-TA**	(1*S*,2*S*)-**CHDA**	90	25	0.75	1	340
L-***α*NCS-TA**	(1*S*,2*S*)-**CHDA**	90	25	0.75	1	350
L-***α*NCS-TA**	(1*S*,2*S*)-**CHDA**	90	25	0.75	1	360
L-***α*NCS-TA**	(1*S*,2*S*)-**CHDA**	90	25	0.75	1	370
L-***α*NCS-TA**	(1*S*,2*S*)-**CHDA**	90	25	0.75	1	380
L-***α*NCS-TA**	(1*S*,2*S*)-**CHDA**	90	25	0.75	1	390
L-***α*NCS-TA**	(1*S*,2*S*)-**CHDA**	90	25	0.75	1	400
L-***α*NCS-TA**	(1*S*,2*S*)-**CHDA**	90	25	0.75	1	410
L-***α*NCS-TA**	(1*S*,2*S*)-**CHDA**	90	25	0.75	1	420
L-***α*NCS-TA**	(1*S*,2*S*)-**CHDA**	90	25	0.75	1	430
L-***α*NCS-TA**	(1*S*,2*S*)-**CHDA**	90	25	0.75	1	440
L-***β*NCS-TA**	(1*R*,2*R*)-**CHDA**	10	25	0.75	1	365
L-***β*NCS-TA**	(1*R*,2*R*)-**CHDA**	20	25	0.75	1	365
L-***β*NCS-TA**	(1*R*,2*R*)-**CHDA**	25	25	0.75	1	365
L-***β*NCS-TA**	(1*R*,2*R*)-**CHDA**	30	25	0.75	1	365
L-***β*NCS-TA**	(1*R*,2*R*)-**CHDA**	40	25	0.75	1	365
L-***β*NCS-TA**	(1*R*,2*R*)-**CHDA**	50	25	0.75	1	365
L-***β*NCS-TA**	(1*R*,2*R*)-**CHDA**	60	25	0.75	1	365
L-***β*NCS-TA**	(1*R*,2*R*)-**CHDA**	75	25	0.75	1	365
L-***β*NCS-TA**	(1*R*,2*R*)-**CHDA**	80	25	0.75	1	365
L-***β*NCS-TA**	(1*R*,2*R*)-**CHDA**	90	25	0.75	1	365
L-***β*NCS-TA**	(1*R*,2*R*)-**CHDA**	80	10	0.75	1	365
L-***β*NCS-TA**	(1*R*,2*R*)-**CHDA**	80	20	0.75	1	365
L-***β*NCS-TA**	(1*R*,2*R*)-**CHDA**	80	30	0.75	1	365
L-***β*NCS-TA**	(1*R*,2*R*)-**CHDA**	80	40	0.75	1	365
L-***β*NCS-TA**	(1*R*,2*R*)-**CHDA**	80	25	0.75	1	365
L-***β*NCS-TA**	(1*R*,2*R*)-**CHDA**	80	25	0.75	0.01	365
L-***β*NCS-TA**	(1*R*,2*R*)-**CHDA**	80	25	0.75	0.1	365
L-***β*NCS-TA**	(1*R*,2*R*)-**CHDA**	80	25	0.75	0.5	365
L-***β*NCS-TA**	(1*R*,2*R*)-**CHDA**	80	25	0.75	1	365
L-***β*NCS-TA**	(1*R*,2*R*)-**CHDA**	80	25	0.75	2	365
L-***β*NCS-TA**	(1*R*,2*R*)-**CHDA**	80	25	0.75	10	365
L-***β*NCS-TA**	(1*R*,2*R*)-**CHDA**	80	25	0.75	1	365
L-***β*NCS-TA**	(1*R*,2*R*)-**CHDA**	80	25	0.1	1	365
L-***β*NCS-TA**	(1*R*,2*R*)-**CHDA**	80	25	0.25	1	365
L-***β*NCS-TA**	(1*R*,2*R*)-**CHDA**	80	25	0.5	1	365
L-***β*NCS-TA**	(1*R*,2*R*)-**CHDA**	80	25	0.75	1	365
L-***β*NCS-TA**	(1*R*,2*R*)-**CHDA**	80	25	1	1	365
L-***β*NCS-TA**	(1*R*,2*R*)-**CHDA**	80	25	1.5	1	365
L-***β*NCS-TA**	(1*R*,2*R*)-**CHDA**	80	25	0.75	1	365
L-***β*NCS-TA**	(1*R*,2*R*)-**CHDA**	80	25	0.75	1	365
L-***β*NCS-TA**	(1*R*,2*R*)-**CHDA**	80	25	0.75	1	330

L-***β*NCS-TA**	(1*R*,2*R*)-**CHDA**	80	25	0.75	1	340
L-***β*NCS-TA**	(1*R*,2*R*)-**CHDA**	80	25	0.75	1	350
L-***β*NCS-TA**	(1*R*,2*R*)-**CHDA**	80	25	0.75	1	360
L-***β*NCS-TA**	(1*R*,2*R*)-**CHDA**	80	25	0.75	1	370
L-***β*NCS-TA**	(1*R*,2*R*)-**CHDA**	80	25	0.75	1	380
L-***β*NCS-TA**	(1*R*,2*R*)-**CHDA**	80	25	0.75	1	390
L-***β*NCS-TA**	(1*R*,2*R*)-**CHDA**	80	25	0.75	1	400
L-***β*NCS-TA**	(1*R*,2*R*)-**CHDA**	80	25	0.75	1	410
L-***β*NCS-TA**	(1*R*,2*R*)-**CHDA**	80	25	0.75	1	420
L-***β*NCS-TA**	(1*R*,2*R*)-**CHDA**	80	25	0.75	1	430
L-***β*NCS-TA**	(1*R*,2*R*)-**CHDA**	80	25	0.75	1	440
L-***β*NCS-TA**	(1*S*,2*S*)-**CHDA**	10	25	0.75	1	365
L-***β*NCS-TA**	(1*S*,2*S*)-**CHDA**	20	25	0.75	1	365
L-***β*NCS-TA**	(1*S*,2*S*)-**CHDA**	25	25	0.75	1	365
L-***β*NCS-TA**	(1*S*,2*S*)-**CHDA**	30	25	0.75	1	365
L-***β*NCS-TA**	(1*S*,2*S*)-**CHDA**	40	25	0.75	1	365
L-***β*NCS-TA**	(1*S*,2*S*)-**CHDA**	50	25	0.75	1	365
L-***β*NCS-TA**	(1*S*,2*S*)-**CHDA**	60	25	0.75	1	365
L-***β*NCS-TA**	(1*S*,2*S*)-**CHDA**	75	25	0.75	1	365
L-***β*NCS-TA**	(1*S*,2*S*)-**CHDA**	80	25	0.75	1	365
L-***β*NCS-TA**	(1*S*,2*S*)-**CHDA**	90	25	0.75	1	365
L-***β*NCS-TA**	(1*S*,2*S*)-**CHDA**	80	10	0.75	1	365
L-***β*NCS-TA**	(1*S*,2*S*)-**CHDA**	80	20	0.75	1	365
L-***β*NCS-TA**	(1*S*,2*S*)-**CHDA**	80	30	0.75	1	365
L-***β*NCS-TA**	(1*S*,2*S*)-**CHDA**	80	40	0.75	1	365
L-***β*NCS-TA**	(1*S*,2*S*)-**CHDA**	80	25	0.75	1	365
L-***β*NCS-TA**	(1*S*,2*S*)-**CHDA**	80	25	0.75	0.01	365
L-***β*NCS-TA**	(1*S*,2*S*)-**CHDA**	80	25	0.75	0.1	365
L-***β*NCS-TA**	(1*S*,2*S*)-**CHDA**	80	25	0.75	0.5	365
L-***β*NCS-TA**	(1*S*,2*S*)-**CHDA**	80	25	0.75	1	365
L-***β*NCS-TA**	(1*S*,2*S*)-**CHDA**	80	25	0.75	2	365
L-***β*NCS-TA**	(1*S*,2*S*)-**CHDA**	80	25	0.75	10	365
L-***β*NCS-TA**	(1*S*,2*S*)-**CHDA**	80	25	0.75	1	365
L-***β*NCS-TA**	(1*S*,2*S*)-**CHDA**	80	25	0.1	1	365
L-***β*NCS-TA**	(1*S*,2*S*)-**CHDA**	80	25	0.25	1	365
L-***β*NCS-TA**	(1*S*,2*S*)-**CHDA**	80	25	0.5	1	365
L-***β*NCS-TA**	(1*S*,2*S*)-**CHDA**	80	25	0.75	1	365
L-***β*NCS-TA**	(1*S*,2*S*)-**CHDA**	80	25	1	1	365
L-***β*NCS-TA**	(1*S*,2*S*)-**CHDA**	80	25	1.5	1	365
L-***β*NCS-TA**	(1*S*,2*S*)-**CHDA**	80	25	0.75	1	365
L-***β*NCS-TA**	(1*S*,2*S*)-**CHDA**	80	25	0.75	1	365
L-***β*NCS-TA**	(1*S*,2*S*)-**CHDA**	80	25	0.75	1	330
L-***β*NCS-TA**	(1*S*,2*S*)-**CHDA**	80	25	0.75	1	340
L-***β*NCS-TA**	(1*S*,2*S*)-**CHDA**	80	25	0.75	1	350
L-***β*NCS-TA**	(1*S*,2*S*)-**CHDA**	80	25	0.75	1	360
L-***β*NCS-TA**	(1*S*,2*S*)-**CHDA**	80	25	0.75	1	370
L-***β*NCS-TA**	(1*S*,2*S*)-**CHDA**	80	25	0.75	1	380

L-***β*NCS-TA**	(1*S*,2*S*)-**CHDA**	80	25	0.75	1	390
L-***β*NCS-TA**	(1*S*,2*S*)-**CHDA**	80	25	0.75	1	400
L-***β*NCS-TA**	(1*S*,2*S*)-**CHDA**	80	25	0.75	1	410
L-***β*NCS-TA**	(1*S*,2*S*)-**CHDA**	80	25	0.75	1	420
L-***β*NCS-TA**	(1*S*,2*S*)-**CHDA**	80	25	0.75	1	430
L-***β*NCS-TA**	(1*S*,2*S*)-**CHDA**	80	25	0.75	1	440

Table S12. Measurement information of entire data for ANN input.

Sample No.	%ee	f_{EtOH} / %	T / ℃	[Host] / mM	Host:Guest / *eq*	λ_{ex} / nm
1	100	80	25	0.75	1	365
2	100	80	25	0.75	1	365
3	100	80	25	0.75	1	365
4	100	80	25	0.75	1	365
5	100	80	25	0.75	1	365
6	100	80	25	0.75	1	365
7	80	80	25	0.75	1	365
8	80	80	25	0.75	1	365
9	80	80	25	0.75	1	365
10	80	80	25	0.75	1	365
11	80	80	25	0.75	1	365
12	80	80	25	0.75	1	365
13	60	80	25	0.75	1	365
14	60	80	25	0.75	1	365
15	60	80	25	0.75	1	365
16	60	80	25	0.75	1	365
17	60	80	25	0.75	1	365
18	60	80	25	0.75	1	365
19	40	80	25	0.75	1	365
20	40	80	25	0.75	1	365
21	40	80	25	0.75	1	365
22	40	80	25	0.75	1	365
23	40	80	25	0.75	1	365
24	40	80	25	0.75	1	365
25	20	80	25	0.75	1	365
26	20	80	25	0.75	1	365
27	20	80	25	0.75	1	365
28	20	80	25	0.75	1	365
29	20	80	25	0.75	1	365
30	20	80	25	0.75	1	365
31	0	80	25	0.75	1	365
32	0	80	25	0.75	1	365
33	0	80	25	0.75	1	365
34	0	80	25	0.75	1	365
35	0	80	25	0.75	1	365
36	0	80	25	0.75	1	365
37	-20	80	25	0.75	1	365
38	-20	80	25	0.75	1	365
39	-20	80	25	0.75	1	365
40	-20	80	25	0.75	1	365
41	-20	80	25	0.75	1	365
42	-20	80	25	0.75	1	365
43	-40	80	25	0.75	1	365
44	-40	80	25	0.75	1	365

45	-40	80	25	0.75	1	365
46	-40	80	25	0.75	1	365
47	-40	80	25	0.75	1	365
48	-40	80	25	0.75	1	365
49	-60	80	25	0.75	1	365
50	-60	80	25	0.75	1	365
51	-60	80	25	0.75	1	365
52	-60	80	25	0.75	1	365
53	-60	80	25	0.75	1	365
54	-60	80	25	0.75	1	365
55	-80	80	25	0.75	1	365
56	-80	80	25	0.75	1	365
57	-80	80	25	0.75	1	365
58	-80	80	25	0.75	1	365
59	-80	80	25	0.75	1	365
60	-80	80	25	0.75	1	365
61	-100	80	25	0.75	1	365
62	-100	80	25	0.75	1	365
63	-100	80	25	0.75	1	365
64	-100	80	25	0.75	1	365
65	-100	80	25	0.75	1	365
66	-100	80	25	0.75	1	365